INVESTIGATION INTO IGBT TRANSIENT CHARACTERISTICS

AND

CALCULATION OF SWITCHING POWER LOSS

A thesis submitted in partial fulfillment of the requirements
for the degree of Bachelor of Science
in the
Department of Electrical and Electronic Engineering

by-

Rifatul Hasan; ID: **12121113**

Sharmin Mustary; ID: **12121167**

Nigar Sultana Bristy; ID: **11321033**

BRAC University

Spring 2016

Declaration

This is to declare that this thesis named "Investigation into IGBT transient voltage characteristics during turn-off operation and reduction of switching power loss" is submitted by the authors listed for the degree of Bachelor of Science in Electrical and Electronics Engineering to the Department of Electrical of Electronics Engineering under the School of Engineering and Computer Science, BRAC University. We hereby affirm that the research work and result was conducted solely by us and no other. Materials of the study and work found by other researchers have been properly referred and acknowledged. This thesis paper, neither in whole nor in part, has been previously submitted elsewhere for appraisal.

Submission Date: 19th April, 2016.

____

Rifatul Hasan

____

Sharmin Mustary

____

Nigar Sultana Bristy

Abstract:

In many power converter applications, analysis of switching power loss of IGBT is considered desirable. In our thesis, the switching behavior is analyzed through investigation into transient anode voltage modeling of Non-Punch Through (NTP) Insulated Gate Bipolar Transistor (IGBT).Parabolic Profile for excess carrier concentration has been compared with the linear one in the baser. With the comparison, Transient turn-off anode voltage is analyzed through parabolic and linear approach. Finally transient switching power loss is estimated through the incorporation of transient current.

Acknowledgement

We express our sincere gratitude to our supervisor, Avijit Das, Lecturer, BRAC University for encouraging and providing us the valuable guidance to complete this research. .He has provided us with necessary materials & instructions which helped us a lot to understand the topic & analyze it better. He has always been there for us to rescue in case of any problems that we might encounter while dealing with this issue. Without his keen supervision, it was virtually impossible for us to finish this report successfully in time. We are grateful to all of our peers and every other individual who has supported, encouraged and lent us hand whenever it was required throughout our research.

Finally, we are very grateful to the Almighty Allah, who has blessed us with knowledge and ability to write this report successfully.

Contents:

List of figures:

List of tables:

Abbreviations

IGBT	Insulated Gate Bipolar Transistor
BJT	Bipolar Junction Transistor
MOSFET	Metal Oxide Semiconductor Field E_ect Transistor
VDMOSFET	Vertical Double diffused MOSFET
RKF	Runge Kutta Fehlberg method
RK4	4th Order Runge Kutta method

Physical Parameters

Ambipolar diffusivities	$D = 18\ cm^2/s$
High level carrier lifetime	$\tau_{HL} = 0.1\mu s$ $= 0.3\mu s$ $= 2.45\mu s$ $= 7.1\mu s$
Supply voltage	$V_{bus} = 400$V
Dielectric constant of Si	$\varepsilon_{Si} = 11.7 \times 8.854 \times 10^{-14}\ F/cm$
Charge of electron	$q = 1.6 \times 10^{-19}$C
Base Doping concentration	$N_B = 2 \times 10^{14} cm^{-3}$
Hole Diffusivity	$D_P = 14 cm^2/s$
Metallurgical base width	$W_B = 9.3 \times 10^{-3} cm$
Device active area	A= 0.1 cm^2
Emitter electron saturation current	$I_{sne} = 6 \times 10^{-14}$A
Intrinsic carrier concentration	n_i =1.45$\times 10^{-10} cm^{-3}$
Electron Mobility	$\mu_n = 1500 cm^2/Vs$
Hole Mobility	μ_p =450 cm^2/Vs
Ambipolar mobility ratio	b=3.3
Total current	$I_T = 10A$

Symbols

A	Device active area	cm^{-3}
$I_{n,}I_p$	electron hole current	A
δp	excess carrier concentration	cm^{-3}
n, p	electron, hole carrier concentration	cm^{-3}
Q	total excess carrier base charge	C
Q_0	steady state base charge	C
P_0	excess carrier concentration at x=0	cm^{-3}
$\emptyset_n, \emptyset_p$	electron,hole quasi-fermi potential	V
E	electric field	V/cm
ε_{Si}	dielectric constant of Si	F/cm
Q	electron charge	C
μ_n, μ_p	electron, hole mobility	cm^{-2}/Vs
$D_n,\ D_p$	electron, hole diffusivity	cm^{-2}/s
τ_{HL}	high level excess carrier lifetime	s
$I_T = I_n + I_p$	Total current	A
$b = \frac{\mu_n}{\mu_p}$	ambipolar mobile ratio	-
D	ambipolar diffusivity	cm^{-2}/s
L	ambipolar diffusion length	cm
x	distance in base from emmiter	cm
W_B	metallurgical base width	cm

W	quasi-neutral base width	cm
W_{bcj}	base-collector depletion width	cm
C_{bcj}	collector-base depletion capacitance	F
N_B	base doping concentration	cm^{-3}
V_{CE}	device anode voltage	V
I_{sne}	emitter electron saturation current	A
V_T	MOSFET channel threshold voltage	V

Dedicated to...
our parents

Chapter 1

Introduction

An Insulated-Gate Bipolar Transistor (IGBT) is a three-terminal power semiconductor device primarily used as an electronic switch which, as it was developed, came to combine high efficiency and fast switching. It switches electric power in many modern appliances: variable frequency drives (VFDs), electric cars, trains, variable speed refrigerators, Uninterruptible Power Supplies (UPS), lamp ballasts, air-conditioners and even stereo systems with switching amplifiers. Since it is designed to turn on and off rapidly, amplifiers that use it often synthesize complex waveforms with pulse-width modulation and low-pass filters. In switching applications modern devices feature pulse repetition rates well into the ultrasonic range—frequencies which are at least ten times the highest audio frequency handled by the device when used as an analog audio amplifier.

Combining the gate behavior of a MOSFET with the conduction behavior of a bipolar transistor produces an Insulated Gate Bipolar Transistor (IGBT).It is a minority-carrier device with high input impedance and large bipolar current-carrying capability. The internal voltage drop of a bipolar transistor when it is turn on is therefore less than that in a power MOSFET with comparable current and blocking voltage. In contrast, a MOSFET can be turned on at the gate with less energy than a bipolar transistor, which requires a relatively high current that has to be maintained throughout the on period. That’s why IGBT is a functional integration of Power MOSFET and BJT devices in monolithic form. The IGBT is also a three terminal (gate, collector, and emitter) full-controlled switch. Its gate/control signal takes place between the gate and emitter, and its switch terminals are the drain and emitter. The high input impedance of power MOSFET allows controlled turn-on and gate controlled turn-OFF [4].

The main advantages of IGBT over a Power MOSFET and a BJT are [5]

- It has a very low on-state voltage drop due to conductivity modulation and has superior on-state current density. So smaller chip size is possible and the cost can be reduced.
- It has lower on-state and switching losses and also lowers thermal impedance.
- Low driving power and a simple drive circuit due to the input MOS gate structure. It can be easily controlled as compared to current controlled devices (thyristor, BJT) in high voltage and high current applications.
- Wide SOA: It has superior current conduction capability compared with the bipolar transistor. It also has excellent forward and reverse blocking Capabilities.

The main drawbacks are:

- A reduction in on-state voltage can cost the IGBT to experience slower switching speed at turn-off. The reason is that while electron flow can be abruptly halted simply by reducing the gate-emitter voltage below the gate threshold voltage (as is the case with the MOSFET), there's still the matter of the holes that are left in the drift and body regions (there's no terminal connection to remove them). The only way to get them out of there is by sweep-out, which is dependent upon voltage across the device and internal recombination. As a result, the device displays a tail current at turn-off until the recombination is complete. This has always been a big drawback for the IGBT.

- Switching speed is inferior to that of a Power MOSFET and superior to that of a BJT. The collector current tailing due to the minority carrier causes the turn-off speed to be slow.
- There is the possibility of latch-up due to the internal PNPN thyristor structure.

Several models have been Parabolic in the literature to describe both the DC and the transient behaviors of the IGBT. These models can be classified into two categories: physics-based and behavioral (compact) models.

The model outlined in this thesis dissertation belongs to the category of physics based models in that the basic semiconductor physics of the IGBT device is used to develop relations between the excess minority carrier's distribution, the anode current(I_T), the base current and the output voltage of the device ($V=V_{CE}=V_{BC}$). There are no exact solutions when considering physics-based modeling approach. Appropriate mathematical representations should be found to roughly approximate the solution. It is possible to reach an exact solution if certain assumptions are met when considering the imposed boundary conditions. The analytical modeling approach uses parameters, which have physical meanings and are related to each other based on the device physics.

Nevertheless, developing a physical model is time consuming. Since there are some simplifying approximations made when developing a physics-based model, accuracy may not be 100%. Furthermore, different structures of the IGBT device or new devices require new modifications or new models.

The analytical model developed by Hefner et al. [3-6] is the most comprehensive in the category of physics-based IGBT model. The general ambipolar transport electron is $I_n(W(t))$ which was used to find an expression for the voltage $\left(\frac{dV(t)}{dt}\right)$. Hefner used the expression of displacement current $I_n(W(t))$ to obtain V(t) for the transient operation of IGBT. Hefner implemented the concept of moving the redistribution current. In transient approach Hefner neither used the steady state expression for p(x) nor did linearize the steady state expression for p(x). Moreover Hefner assumed $C_{bcj}(t)$ to be constant with time, which is not so in reality.

Trivedi et al. [7] provided a numerical solution to obtain $\frac{dV(t)}{dt}$in terms of the total current I_T during the turn-off for hard and soft switching IGBT application. The sweeping out action of the excess carriers in the drift region due to the widening of the collector-base depletion was used to obtain $\frac{dV(t)}{dt}$expression. Since W(t) shrinks due to the widening of the depletion region in the collector-base, the charges are forced to be taken away and $I_h = qp(X)v(X) = qp(X)\frac{dW(t)}{dt}$

Ramamurthy et al. [8] Parabolic an analytical expression for the voltage variation with time$\frac{dV(t)}{dt}$for the turn-off of the IGBT. The simple expression for the variation of the internal charges and the boundary conditions with voltages is a non-linear one. For the turn- off analysis, Ramamurthy linearized the steady state carrier concentration expression p(x). Ramamurthy used a positive value for $\frac{dW(t)}{dt}$ instead of a negative sign, which contradicts Which contradicts the equality $W(t)= W_B-W_{bcj}(t)$.

Fatemizadeh et al. [9] developed a semi-empirical model for IGBT in which the DC and the transient current transport mechanisms of the device were approximated by simple analytical equations. The model equations of the IGBT were installed on the PSPICE simulator using analog behavioral modeling tools. However, the accuracy of the model is limited by the fact that the analytical semi-empirical model is over simplified.

Yue et al. [10] presented an analytical IGBT model for the steady state and transient applications including all levels of free carrier injection in the base region of the IGBT. The authors have shown that the low and high injection models significantly overestimate the IGBT current at large and small bias conditions respectively.

Kraus et al. [11] considered an NPT IGBT with a higher charge carrier lifetime and lower emitter efficiency. The injection of electrons into the emitter of the IGBT instead of carrier recombination in the base determined the I-V characteristics. The anode holecurrents and the emitter hole currents are assumed constant. Due to his neglecting of the recombination in the base, a linear charge distribution instead of the hyperbolic function was derived.

Kuo et al. [12] derived an analytical expression for the forward conduction voltage (V_F) for NPT and PT IGBTs taking into account the conductivity modulation in the base of the IGBT. The MOSFET section has not been included in the analysis. Since I_{MOS} controls the turn-off process of the IGBT, the MOSFET section should have been included.

Sheng et al. [13] solved the two dimensional (2-D) carrier distribution equations to model the forward conduction voltages, which can be used in circuit simulation and device analysis for (DMOS IGBT). The drawback of this modeling approach is that it contains complex terms that would impose some requirements on the simulator.

Sheng et al. [14] reviewed IGBT models published in the literature; he then analyzed, compared and classified models into different categories based on mathematical type, objectives, complexity and accuracy. Although [14] claimed that many mathematical models are accurate and able to predict electrical behavior in different circuit conditions compared to the behavioral models, it failed to provide a comprehensive physical model for understanding the device mechanisms.

Leturcq [15] Parabolic a simplified approach to the analysis of the switching condition in IGBT. The approach was based on a new method for solving the ambipolar diffusion equation taking the moving depletion boundary in the base into consideration. This paper helped in understanding the switching process in IGBT.

The above literature survey dealt mainly with IGBT having planar structures, namely the Non-Panch Through (NPT) and the Punched Through (PT) IGBT, although other structures were

Parabolic in the literature to improve the I-V characteristics of IGBTs, temperature operation or develop better physics-based models.

Chapter 2 describes the basic structure of an IGBT and provides a description of the IGBT operation. In addition, the chapter introduces the ambipolar transport analysis, which is the key feature in modeling the IGBT device. The conclusion of the chapter highlights the basic tools for the analysis: the steady state and the transient operation of an IGBT. Chapter 3 covers the literature review analysis of the most important transient modeling of IGBT. Chapter 4 introduces new physics-based models for NPT IGBT wherein the steady state part of the model is derived by solving the ambipolar diffusion equation in the base. The turn-off transient part of the model is based on the availability of a new expression for excess carrier charge distribution in the base. The transient voltage is obtained numerically from this model. Alternatively we have Parabolic and implemented an analytical solution for the transient voltage. In addition, the power dissipation P(t) and the switching losses E_{off} in IGBT are calculated and simulated for different device carrier lifetimes.

1.1 Device Evolution: BJT, MOSFET and IGBT

The bipolar transistor was the only "real" power transistor until the MOSFET came along in the 1970's. The bipolar transistor requires a high base current to turn on, has relatively slow turn-off characteristics (known as current tail), and is liable for thermal runaway due to a negative temperature co-efficient. In addition, the lowest attainable on-state voltage or conduction loss is governed by the collector-emitter saturation voltage $V_{CE(SAT)}$.

The MOSFET, however, is a device that is voltage- and not current-controlled. MOSFETs have a positive temperature co-efficient, stopping thermal runaway. The on-state-resistance has no theoretical limit; hence on-state losses can be far lower. The MOSFET also has a body-drain diode, which is particularly useful in dealing with limited freewheeling currents. All these advantages and the comparative elimination of the current tail soon meant that the MOSFET became the device of choice for power switch designs.

Then in the 1980s the IGBT came along. The IGBT is a cross between the bipolar and MOSFET transistors. Early versions of the IGBT are also prone to latch up, but nowadays, this is pretty well eliminated. Another potential problem with some IGBT types is the negative temperature co-efficient, which could lead to thermal runaway and makes the paralleling of devices hard to effectively achieve. This problem is now being addressed in the latest generations of IGBTs that are based on "non-punch through" (NPT) technology. This technology has the same basic IGBT structure but is based on bulk-diffused silicon, rather than the epitaxial material that both IGBTs and MOSFETs have historically used.

Table 1.1.1: Comparison among MOSFET, IGBT and BJT:

Characteristics	MOSFET	IGBT	BJT
Type of drive	voltage	voltage	current
Drive power	Minimal	Minimal	Large
Drive complexity	simple	simple	High (large positive and negative currents required)
Current density for given voltage drop	High at low voltage. Low at high voltages.	Very high(small trade-off with switching speed)	Medium (severe trade-off with switching speed)
Switching losses	Very low	Low to medium (depending on trade-off with conduction losses)	Medium to high (depending on trade-off with conduction losses)

1.2 Significance of IGBT:

In 1979, a typical cross between the bipolar and MOSFET transistors came in the light having the name IGBT which had the output switching and conduction characteristics of a bipolar transistor but was voltage-controlled like a MOSFET. In general, this means it has the advantages of high-current handling capability of a bipolar with the ease of control of a MOSFET.

However, many high voltage applications do not take advantage of the superior switching capabilities of MOSFETs, due to EMI constraints and stray inductances. In these applications IGBT can be an appealing alternative for a number of reasons:

- Much lower conduction losses that are substantially constant over temperature.
- Smaller die area with lower input capacitance, simpler gate drive and lower cost.
- Smooth di/dt and dv/dt with minimal EMI signature and low overshoots.
- The diode co-packaged with the IGBT has much superior switching characteristics than the integral body diode of high voltage MOSFET and generates lower current spikes. This is a distinct advantage in those topologies that rely on an anti-parallel diode.

Nowadays, IGBT is used as an electronic switch in many modern appliances: variable-frequency drives (VFDs), electric cars, trains, variable speed refrigerators, air-conditioners and even stereo systems with switching amplifiers. Moreover, today a high efficiency matrix converter can be achieved by using the RB-IGBT, which has a great possibility to replace the conventional DC-linked-type circuits.

Chapter 2

Basic Principles of IGBT

2.1 Basic Structure

2.1.1 Cross sectional structure

The cross section of a typical IGBT has been shown in below the figure 2.1. The structure of the device is similar to that of a vertical double diffused MOSFET with the exception that a highly doped p-type substrate is used in lieu of a highly doped n-type drain contact in the vertical double diffused MOSFET. A lightly doped thick n-type epitaxial layer ($N_B = 10^{14} cm^{-3}$) is grown on top of the p-type substrate to support the high blocking voltage in the reverse bias mode state. A highly doped p-type region ($N_A = 10^{19} cm^{-3}$) is added to the structure to prevent the activation of the PNPN thyristor during the device operation. The power MOSFET is a voltage-controlled device that can be manipulated with a small input gate current flow during the switching transient. This makes its gate control circuit simple and easy to use.

A highly doped n^+ buffer layer could also be added on top of the highly doped p^+ substrate. This layer helps in reducing the turn-off time of the IGBT during the transient operation. The IGBT with a buffer layer is called a punch through PT IGBT while the IGBT without buffer layer is called a non-punch through NPT IGBT.

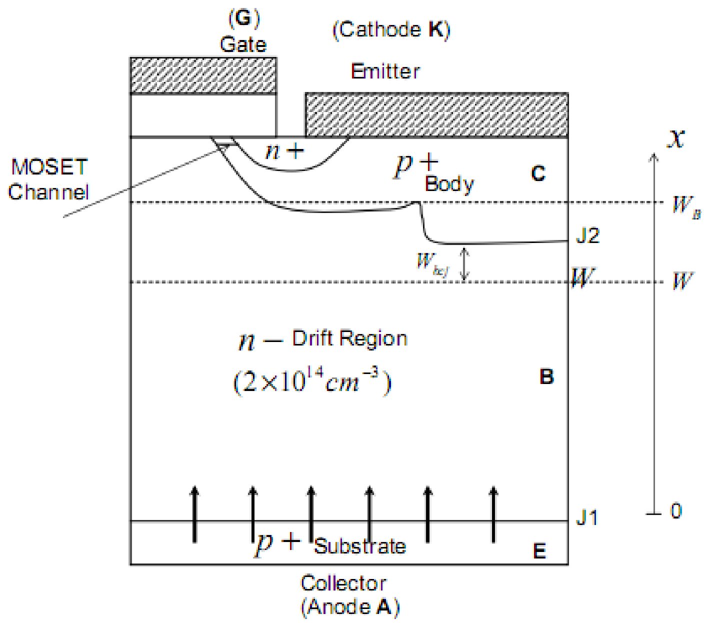

Figure 2.1: A cross section schematic of the IGBT half-cell [1]

2.1.2 NPT and PT IGBT

PT IGBTs were the first IGBT available on the market. In the case of PT IGBT, the epilayer is not as thick (less thick) as NPT IGBT because a n^+ layer is placed over the p^+ layer. It is very likely to have punched through the J2 junction to the J1 junction. This n^+ layer can handle some of the punch through hand act as a shield to the J1 junction. This n^+ buffer layer occupies some spaces in the base of IGBT, which leaves less space for the total charges in the base region during the IGBT on state (turn-on) operation. As a result, these charges are removed by the n^+ layer more quickly when switching occurs. This n^+ layer is a recombination center which helps holes get recombined with electrons before reaching the base region and fewer holes, as a result, will be injected into the base region (lower efficiency). As a result, the carrier lifetime is reduced and the switching frequency is increased. However, since fewer carriers are injected into the base region compared to the NPT IGBT, the conductivity modulation (explained later) is reduced (higher base resistance) and the on-state voltage is increased. The trade-off between the reduced turn-off time and the increased on-state voltage should be accounted for. For NPT IGBT considered in this thesis dissertation, the epilayer thickness is thick enough since no n^+ layer is introduced on top of the highly doped p^+ layer substrate. Because the thickness of the n^- layer is greater than PT IGBT, the resistance is high in this region and, as a result, a higher reversed voltage can be sustained when J2 is reversed biased. The punch through of the J2 to the J1 is less likely to occur, i.e. a non-punch through situation. If the punch through occurs, then the IGBT breakdown voltage will be degraded causing the deviceto break down. When the emitter base junction J1 is forward biased and the gate voltage is greater than the threshold voltage V_T ; injection of holes from the p^+ substrate is increased. The resistance of the n- layer is reduced when the injected hole density becomes much greater than the background doping ($n^- = N_B$) .

The turn-off time of the NPT IGBT is longer than the PT IGBT because the removal of so many stored charges in the base region is slow due to the absence of recombination centers. Carriers do not recombine as fast, which means they have longer lifetimes. The NPT IGBT is more efficient than the PT ones since more charges are injected from the p^+ layer to the n^-. The injected holes do not get recombined as fast as in PT IGBT, which has an n^+ buffer layer on top of the p^+ layer. Figure 2.2 shows cross section of PT and NPT IGBT

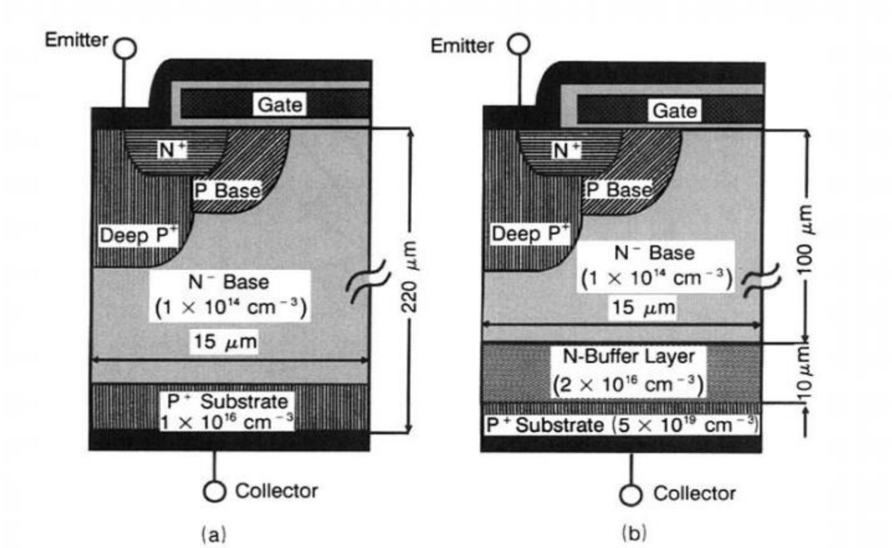

FIGURE 2.2: Cross section structure of (a) NPT IGBT and (b) PT IGBT [2]

The PT structure has an extra buffer layer which performs two main functions:

(i) Avoids failure by punch-through action because the depletion region expansion at applied high voltage is restricted by this layer,

(ii) Reduces the tail current during turn-off and shortens the fall time of the IGBT because the holes are injected by the P^{+} collector partially recombine in this layer

• The NPT IGBTs, which have equal forward and reverse breakdown voltage, are suitable for AC applications.

• The PT IGBTs, which have less reverse breakdown voltage than the forward breakdown voltage, are applicable for DC circuits where devices are not required to support voltage in the reverse direction.

Fig. 2.3 shows the Doping Concentration & Electric Field distribution of NPT & PT IGBT.

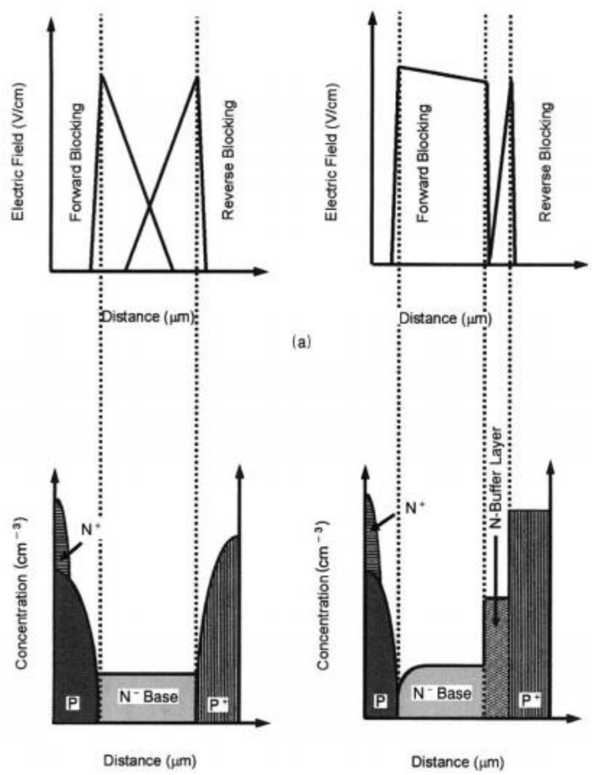

FIGURE 2.3: Doping Concentration & Electric Field Distribution (a)NPT IGBT & (b)PT IGBT [2]

Table 2.1.2.1: Characteristic comparison of NPT and PT IGBT

Parameter	NPT	PT
Switching loss	Medium	Low
Conduction loss	Medium	Low
Paralleling	Easy	Difficult
Short circuit test	Yes	Limited; high gain

2.2 Principles of operation of IGBT

2.2.1 Equivalent circuit of IGBT

Based on the structure, an equivalent circuit of IGBT can be shown in Fig. 2.4.

It consists of a PNP transistor (BJT) & a n channel MOSFET. The p^+ substrate, n^- epilayer& p^+ body forms the PNP transistor. The p-type substrate is the emitter for BJT and is the anode terminal of the device. When the p substrate is forward biased ($V_{EB} > 0$), the minority carrier injection causes transistor current I_T flowing from the anode region. This current has two parts at the Base-

Electron current (I_n (W)).

Hole current (I_p(W)).

The Anode to Cathode voltage (V_{AC}) can be represented by

$$V_{AC} = V_{EB} + V_{BC}$$

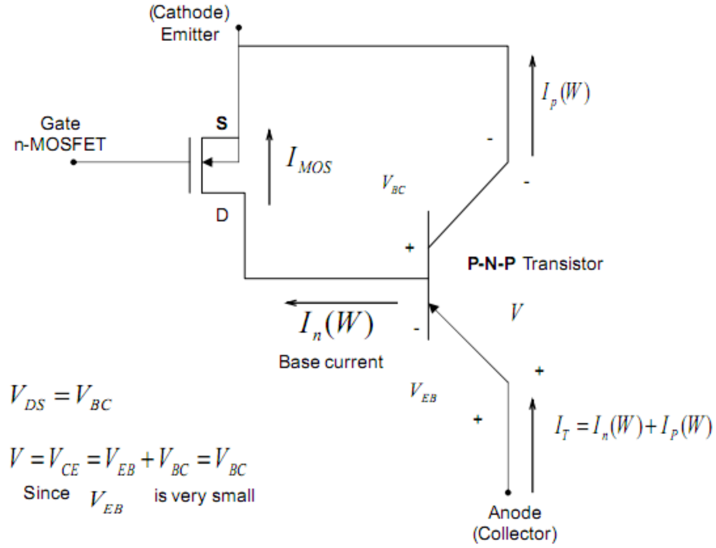

FIGURE 2.4: The equivalent circuit model of IGBT [1]

V_{EB}=Bipolar Emitter to Base voltage.

V_{BC}=Base to Cathode voltage.

Basically V_{DS} of MOSFET & V_{BC} are same. Since V_{EB} is very small, we can write V_{AC}= V_{BC}

From the equivalent circuit, a circuit symbol can be formed which is shown in Fig. 2.5. It has three parts-

Collector (C) which is the anode terminal of IGBT.

Gate (G) which is the Gate terminal of MOSFET.

Emitter (E) which is the cathode terminal of IGBT.

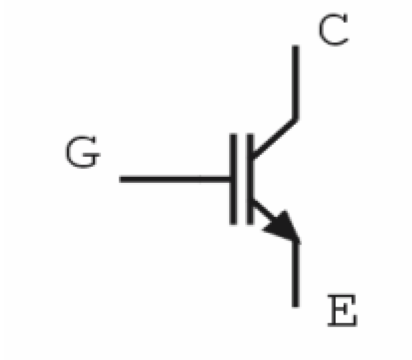

FIGURE 2.5: Circuit symbol of IGBT [1]

2.2.2 IGBT Operation

When a positive gate voltage greater than the threshold voltage (V_T) is applied, electrons are attracted from the p^+ body towards the surface under the gate. These attracted electrons will invert the p^+ body region directly under the gate to form an n channel. A path is formed for charges to flow between the n^+ source and the n^- drift region.

When a positive voltage is applied to the anode terminal of the IGBT, the emitter of the IGBT section is at higher voltage than collector. Minority carriers (holes) are injected from the emitter (p^+region) into the base (n^-drift region). As the positive bias on the emitter of the BJT part of the IGBT increases, the concentration of the injected hole increases as well. The concentration of the injected holes will eventually exceed the background doping level of the n^-drift region; hence the conductivity modulation phenomenon. The injected carriers reduce the resistance of the n^-drift region and, as a result, the injected holes are recombined with the electrons flowing from the source of the MOSFET to produce the anode current (on state).

When a negative voltage is applied to the anode terminal, the emitter-base junction is reversed biased the current is reduced to zero. A large voltage drop appears in the n^-drift region since the depletion layer extends mainly into that region.

The MOSFET gate voltage controls the IGBT switching action. The turn-off takes place when the gate voltage is less than the threshold voltage (V_T). The inversion layer at the surface of the p^+body under the gate cannot be kept and therefore no electron current is available in the MOSFET channel while the remaining minority carriers of holes, which were stored during the on state of the IGBT, require some time in order to be removed or extracted.

The switching speed of the IGBT device depends upon the time it takes for the removal of the stored charges in the n^-drift region which were built up during the on state current conduction (IGBT turn-on case).

2.3 Basic Tools for Operation

The Physics-based modeling approach is used in this discussion to better understand the effect of the carriers on the IGBT characteristics. The following points have to be taken into account in performing the analysis

- The carrier distribution in the n-drift region of the IGBT is described by the ambipolar diffusion equation because of the high level injection of holes in this region($p(x) >> NB$.

$$\frac{\partial^2 p(x)}{\partial x^2} = \frac{p(x)}{L^2} + \frac{1}{D}\frac{\partial \mathrm{p(x)}}{\partial \mathrm{x}}$$

Where,

N_B = Base background doping concentration

$p(x)$ = Hole concentration

$L = \sqrt{D\tau_{HL}}$

- Transport of the bipolar charge is assumed to be one-dimensional (1-D) for the ease of analysis.

- The emitter region of the BJT part of the IGBT has a very high doping, concentration level ($p^{+} >> 10^{18} cm^{-3}$). This region acts like recombination centers for minority carriers coming from the lightly doped base region (electron in this case).
- The space charge region, which is depleted of minority carriers, supports the entire voltage drop across the collector-base terminals based on Poisson's equation. The effect of mobile carriers in the depletion region is not accounted for in this dissertation.

2.3.1 The Steady State Analysis

The equivalent circuit model and 1-D coordinate system of Fig. 2.6 is used in the modeling approach of the NPT IGBT analysis. From this figure, I_T is the IGBT total current, I_p is the hole current of the BJT and I_n is the base or MOS electron current.

I_T can be expressed in several ways:

$$I_T = I_p(x = 0) + I_n(x = 0) \quad (2.1)$$

$$I_T = I_p(x = W) + I_p(x = W) \quad (2.2)$$

$$I_T = I_p(\mathrm{x}) + = I_n(\mathrm{x}) \quad (2.3)$$

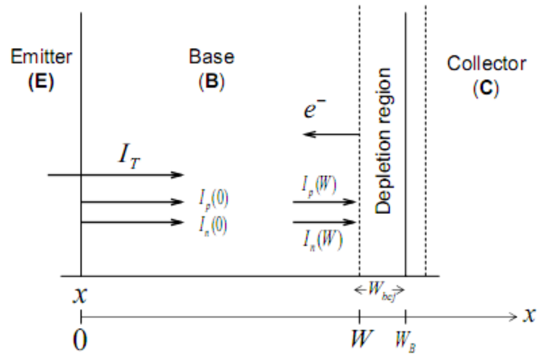

FIGURE 2.6: 1-D coordinate system used in the modeling of the NPT IGBT [1]

The IGBT operates under low gain and high level injection conditions. The current equations are as

$$J_n = nq\mu_n + qD_n \frac{\partial n(x)}{\partial x} \tag{2.4}$$

$$J_n = pq\mu_p - qD_p \frac{\partial p(x)}{\partial x} \tag{2.5}$$

Where J_n is the electron current & J_p is the hole current.

The first terms in equations & are due to drift component while the second terms are due to diffusion component.

When the excess carrier concentration is larger than the background concentration the transport of electrons and holes are coupled by the electric field in the drift terms of the transport equations. The minority carrier current density J_n cannot be neglected and ends up affecting the majority carrier current density J_p. Hence equations 2.4 & 2.5 cannot be decoupled.

The total current density is given by,

$$J_T = J_n + J_p$$

$$= (nq\mu_n + pq\mu_p)E + q\left(D_n \frac{\partial n(x)}{\partial x} - D_p \frac{\partial p(x)}{\partial x}\right)$$

Substituting for the electric field from the above equation into equation (2.4) yields

$$J_n = \left[\frac{nq\mu_n}{nq\mu_n + pq\mu_p}\right] J_T + q\frac{\partial n}{\partial x}\left[\frac{nq\mu_n D_P + pq\mu_p D_P}{nq\mu_n + pq\mu_p}\right]$$

An ambipolar diffusion coefficient D is defined as

$$D = \left[\frac{nq\mu_n D_P + pq\mu_p D_P}{nq\mu_n + pq\mu_p}\right]$$

The expression for J_n can be rearranged & rewritten as

$$J_n = \left[\frac{b}{1+b}\right] J_T + qD\frac{\partial n}{\partial x} \tag{2.6}$$

Where b $= \frac{\mu_n}{\mu_p}$

Repeating the same procedure starting with equation (2.6), J_p is obtained

$$J_p = \left[\frac{b}{1+b}\right] J_{T} - qD\frac{\partial p}{\partial x} \tag{2.7}$$

Where J_T is the total current density= $J_n + J_p$ & assuming $n=p$

The excess hole carrier distribution p(x) can be obtained by solving the steady state hole continuity equation

$$\frac{\partial^2 p(x)}{\partial x^2} = \frac{p(x)}{L^2} \tag{2.8}$$

Considering the coordinate system given in Fig. 2.1, the boundary conditions for the excess hole carrier distribution are

$$p(x=0) = P_0 \tag{2.9}$$

$$p(x\text{=W})\text{=}0 \tag{2.10}$$

Equation (2.10) results from the collector-base junction being reversed biased for forward condition and equation (2.10) reflects that emitter-base junction is forward biased.

P_0 is the excess carrier concentration at x=0, W(t) is the quasi-neutral base width given by

$$W\text{=}W_B - W_{bcj} \tag{2.11}$$

Where W_B is the metallurgical base width and W_{bcj} is the collector-base depletion width. We know, Poisson's equation

$$\frac{d^2V}{dx^2} = \frac{qN_B}{\epsilon_{Si}} \tag{2.12}$$

Solving Poisson's equation yields an expression for the collector-base junction depletion width as ,

$$W_{bcj} = \sqrt{\frac{2\epsilon_{Si} V_{bc}}{qN_B}}$$

Where N_B is the doping concentration of the lightly doped region of the IGBT and ϵ_{Si} is the dielectric constant of silicon. The junction voltage V_{bcj} $=V=V_{bc}+V_{bi}$ is the collector-base junction voltage drop of the BJT part of the IGBT and V_{bi} is the built in potential. Hence from figure 2.6

$$W= W_B - \sqrt{\frac{2\epsilon_{Si} V}{qN_B}}$$

where $V=V_{bc}=V_{BE}=V_A$ is the collector-base voltage that appears across the drift region.

2.3.2 Transient Operation of IGBT

While the turn-on time of the IGBT is quite fast, the turn-off time can be slow because of the open base of the PNP transistor during the turn-off period. Fig. 2.7 shows the typical IGBT turn-off transient where I_T (0^+) is the current after the initial rapid fall. The initial rapid drop in the anode current is due to the sudden removal of the MOS channel. This is followed by a slower decay due to the removal of the carriers stored in the lightly doped layer (n^-). The turn-off process is initiated when we lower the gate voltage to a value lower than threshold voltage(V_T). This removes the formed electron channel from under the gate and blocks the MOS component of the current I_{MOS}. $I_{MOS}=I_n(W\ )=0$ in this case and the collector-base voltage V_{bc} increases resulting in a widening of the depletion region at the n^- (base-collector side or source of MOSFET).

The relation between $I_T(0^-)$ and $I_T(0^+)$ is through β_{tr}. It is the ratio of the current immediately after the initial rapid fall to the magnitude of the fall and is shown along with the ratio of W(t) to *L (W(t)/L)* in the appendices.

The switching losses of the IGBT are dominated by the losses, which occur during the much slower second phase of the turn-off period transient. This is because of the time required removing or extracting the injected carriers in this phase. This is a major disadvantage of the IGBT device as it suffers from high-switching losses. This can be overcome by reducing the lifetime of the carriers in the base through recombination of extraction processes s quickly as possible before the device reaches its blocking voltage state.

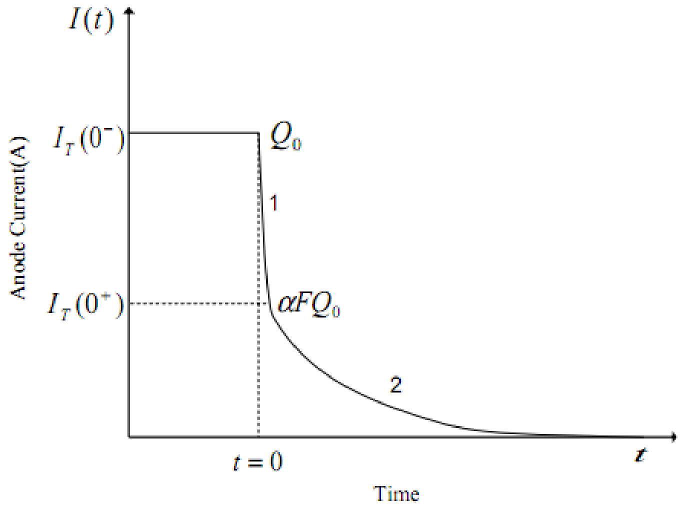

FIGURE 2.7: Typical IGBT turn-off transient showing turn-off phases (1 & 2) [1]

The collector-base junction is reversed biased and its depletion region widens during the turn-off the IGBT. When the IGBT is on, the status of the base-collector junction is reversed biased as can be seen from Fig. 2.4. When the IGBT is off, the status of the base-collector junction is reversed biased and V_{bc} is increased leading to the increment of the depletion region since the current decreases. The widened region supports the entire voltage drop across the device as mentioned previously based on Poisson's equation. Since the quasi-neutral base width of the IGBT changes with time and decreases with the increase of V_{bc}.. we can find an expression for the rate of rise of the voltage across the device $\frac{dV(t)}{dt}$ (varying ofthe output voltage) during the switching-OFF of the IGBT from the collector-base junction depletion width W_{bcj} expression as shown. From $W_{bcj}=\sqrt{\frac{2\epsilon_{Si}V_{bc}}{qN_B}}$ and the fact that $W(t)=W_B-W_{bcj}(t)$ if we take the time derivative of $W_{bcj}(t)$, we get

$$\frac{dW_{bcj}(t)}{dt}=\sqrt{\frac{\epsilon_{Si}}{2qN_{BV(t)}}}\frac{dV(t)}{dt}$$

This equation shows the time rate of the change of the quasi-neutral base width (W(t)) that covers almost all the length across the drift region during the turn-off since the collector-base junction is reversed biased.

Chapter 3

Literature review of some transient modeling of IGBT:

Several models have been Parabolic in the literature to describe both the DC and the transient behaviors of the IGBT. In this section, we have reviewed the most popular model Parabolic by Allen R. Hefner.

3.1 Approaches Taken By Allen R. Hefner

3.1.1 Expression for transient voltage & stored charge decay

In Hefner's [3] [6] transient modeling approach, the general ambipolar trans-port electron current expression

$$I_n(W(t)) = \frac{I_T(t)}{1+\frac{1}{b}} + qAD\frac{\partial n(x,t)}{\partial x}$$

Which was used to find an expression for the voltage rise (dV(t)/dt). $I_n(W(t))=I_{MOS}$ as shown in Fig. 2.6 and it is important since it controls the operation of IGBT.

Since the reverse bias on junction J_2 in Fig. 1 does not increase rapidly and the depletion capacitance of junction $J_2$is partially charged in a short period of time, I_{MOS} current is instantaneous. An expression for I_{MOS} can be obtained if we consider the collection-base junction depletion capacitance as in Fig. 3.1.

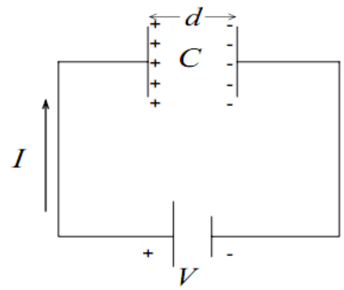

FIGURE 3.1: The collector-base depletion capacitance formation [1]

For the voltage V(t) between the plates, the charge per unit area q =$\frac{\in_{Si} V(t)}{d}$,where d is the distance between the plates and the rate of q change is ,

$$\frac{dq}{dt} = I(current)$$

As we know $q(t) = C_{bcj}(t)V(t)$, so

$$\frac{dq}{dt} = \frac{d}{dt}\left[C_{bcj}(t)V(t)\right]$$

$$=V(t)\frac{d_{bcj}(t)}{dt}+C_{bcj}(t)\frac{dV(t)}{dt}$$

and in terms of the junction capacitance of the reverse biased junction, the displacement current In(W(t)) is

$$I_n(W) = V(t)\frac{d_{bcj}(t)}{dt}+C_{bcj}(t)\frac{dV(t)}{dt} \qquad (3.1)$$

The first term on the right hand side of the equation (3.1) was ignored by Hefner. The rate of change of $C_{bcj}(t)$ should be included in calculating the displacement current since the capacitance varies with time as the depletion width changes with voltage. From equation (2.6) and the fact that J = I/A, where A is the device active area,

$$I_n(W(t)) = \frac{I_T(t)}{1+\frac{1}{b}} + qAD\frac{\partial p(x,t)}{\partial x}$$

And from Hefner's approach

$$I_n(W(t)) = C_{bcj}(t)\frac{dV(t)}{dt} = \frac{2qAD_p}{1+\frac{1}{b}}\frac{\partial p(x,t)}{\partial x}$$

$$\text{Or,} \left(1+\frac{1}{b}\right) C_{bcj}\ \frac{dV(t)}{dt} = I_T + 2qAD_p\ \frac{\partial p(x,t)}{\partial x} \qquad (3.2)$$

Hefner used equation (3.2) to obtain V(t) for the transient operation of IGBT. He implemented the concept of moving the redistribution current. In his transient approach, he neither used the steady state expression for p(x) nor did he linearize the steady state expression for p(x). Moreover he assumed $C_{bcj}(t)$ to be constant with time, which is not so in reality.

His p(x) expression consists of two parts,

$$p(x) = P_0\left[1-\frac{x}{W(t)}\right] - \frac{P_0}{W(t)D}\left[\frac{x^2}{2}-\frac{W(t)x}{6}-\frac{x^3}{3W(t)}\right]\frac{dW(t)}{dt} \qquad (3.3)$$

From equation (2.6) & (3.3)

$$I_n(W(t)) = \frac{bI_T(t)}{1+b} + qAD\frac{\partial p(x)}{\partial x}$$

$$\text{Or,} I_n(W(t)) = \frac{I_T(t)}{1+\frac{1}{b}} + \frac{2qAD_P}{1+\frac{1}{b}}\frac{\partial p(x)}{\partial x} \qquad (3.4)$$

and instead of equation (3.1), Hefner applied $I_n(W(t)) = C_{bcj}(t)\,\frac{dV}{dt}$ in his approach. Integrating equation (3.3) in the base and multiplying by qA, the total charge Q,

$$Q = qA\int_0^W p(x)dx$$

$$= qA\left[x-\frac{x^2}{2W(t)}\right] - \frac{P_0}{W(t)D}\left[\frac{x^3}{6}-\frac{W(t)x^2}{12}-\frac{x^4}{12W(t)}\right]\frac{dW(t)}{dt}$$

$$= qA\left[P_0(W(t)-\frac{W(t)}{2})-\frac{x^2}{2W(t)}\right] - \frac{P_0}{W(t)D}\left[\frac{x^3}{6}-\frac{W(t)x^2}{12}-\frac{x^4}{12W(t)}\right]\frac{dW(t)}{dt}$$

$$= \frac{qAP_0W(t)}{2} - \frac{qA}{P_0WD}\times 0$$

$$=\frac{qAP_0W(t)}{2} \qquad (3.5)$$

as can be seen $\frac{dW(t)}{dt}$ has no effect on Q calculation.

We can find $\frac{\partial p(x)}{\partial x}$ from equation (3.3) as when x=W(t)

$$\frac{\partial p(x)}{\partial x}=\frac{P_0}{W(t)}-\frac{P_0}{W(t)D}\left[\frac{2x}{2}-\frac{W(t)}{6}-\frac{3x^2}{W(t)}\right]\frac{dW(t)}{dt}$$

When *x=W(t)*

$$\frac{\partial p(x)}{\partial x}=\frac{-P_0}{W(t)}-\frac{P_0}{W(t)D}\left[W(t)-\frac{W(t)}{6}-W(t)\right]\frac{dW(t)}{dt}$$

$$\frac{\partial p(x)}{\partial x}=\frac{-P_0}{W(t)}-\frac{P_0}{6D}\frac{dW(t)}{dt}$$

The hole current is $-qA\frac{\partial p(x)}{\partial x}$ and from the above equation

$$-qAD\frac{\partial p(x)}{\partial x}=\frac{qAD\,P_0}{W(t)}-\frac{qAP_0D}{6D}\frac{dW(t)}{dt}$$

$$=\frac{qAD\,P_0}{W(t)}-\frac{qAP_{0D}}{6D}\frac{dW(t)}{dt}$$

As Q=$\frac{qAP_0W(t)}{2}$,from above equation

$$-qAD\frac{\partial p(x)}{\partial x}=\frac{2QD}{W^2(t)}-\frac{Q}{3W(t)}\frac{dW(t)}{dt} \qquad (3.6)$$

The first term on the right hand side of equation (3.6) is categorized by Hefner asthe charge control component and the second term is categorized as the moving boundary redistribution component of the hole current.

From equation (3.4) and (3.6)

$$I_n(W(t)) = C\frac{dV(t)}{dt} = \frac{I_T(t)}{1+\frac{1}{b}} - \frac{4QD_P}{\left(1+\frac{1}{b}\right)W^2(t)} + \frac{Q}{3W(t)}\frac{dW(t)}{dt}$$

This equation can be expressed in a different way if in $-qA\frac{\partial P(x)}{\partial x}$ equation (3.6) is modified as

$$-qAD\frac{\partial p(x)}{\partial x} = \frac{-2qAD_p}{1+\frac{1}{b}}\frac{\partial p(x)}{\partial x}\frac{2QD}{W^2(t)} - \frac{Q}{3W(t)}\frac{dW(t)}{dt}$$

$$-2qAD_p\frac{\partial p(x)}{\partial x} = \frac{2QD}{W^2(t)}\left(1+\frac{1}{b}\right) - \frac{Q}{3W(t)}\left(1+\frac{1}{b}\right)\frac{dW(t)}{dt}$$

$$-2qAD_p\frac{\partial p(x)}{\partial x} = \frac{4D_pD_nQ}{W^2(t)(D_p+D_n)}\left(1+\frac{1}{b}\right) - \frac{Q}{3W(t)}\left(1+\frac{1}{b}\right)\frac{dW(t)}{dt}$$

$$-2qAD_p\frac{\partial p(x)}{\partial x} = \frac{4D_pQ}{W^2(t)} - \frac{Q}{3W(t)}\left(1+\frac{1}{b}\right)\frac{dW(t)}{dt} \tag{3.7}$$

From equation (3.4), we have

$$I_n(W(t)) = C\frac{dV}{dt} = \frac{I_T(t)}{1+\frac{1}{b}} + \frac{2qAD_P}{1+\frac{1}{b}}\frac{\partial p(x)}{\partial x}$$

That can be rearranged as,

$$\left(1+\frac{1}{b}\right)C(t)\frac{dV}{dt} = I_T(t) + \frac{2qAD_P}{1+\frac{1}{b}}\frac{\partial p(x)}{\partial x}$$

Now using equation (3.7), and the fact that

$$C(t) = C_{bcj}(t) = \frac{A\varepsilon_{Si}}{W_{bcj}(t)} = A\sqrt{\frac{2\varepsilon_{Si}N_B}{2V(t)}}\ and\ \frac{dW(t)}{dt} = \frac{-C}{qAN_B}\frac{dV(t)}{dt}$$

the above equation yields,

$$\left(1+\frac{1}{b}\right)C_{bcj}(t)\frac{dV(t)}{dt} = I_T(t) - \frac{4D_pQ}{W^2(t)} - \frac{Q}{3W(t)}\left(1+\frac{1}{b}\right)\frac{dW(t)}{dt}$$

$$\text{Or,} C_{bcj}(t)\frac{dV(t)}{dt}\left[1+\frac{Q}{3qAW(t)N_B}\right] = \frac{I_T(t)-\frac{4D_pQ}{W^2(t)}}{\left(1+\frac{1}{b}\right)}$$

$$\frac{dV(t)}{dt} = \frac{I_T(t)-\frac{4D_pQ}{W^2(t)}}{C_{bcj}(t)\left(1+\frac{1}{b}\right)\left[1+\frac{Q}{3qAW(t)N_B}\right]} \tag{3.8}$$

Where $I_T(t) = I_T(0^-)$ for large inductive loads and $I_T(t) = \frac{4D_pQ(t)}{W^2(t)}$[Appendix A] forthe constant anode voltage in which$\frac{dV(t)}{dt} = 0$ indicating that the voltage W(t) are constants.

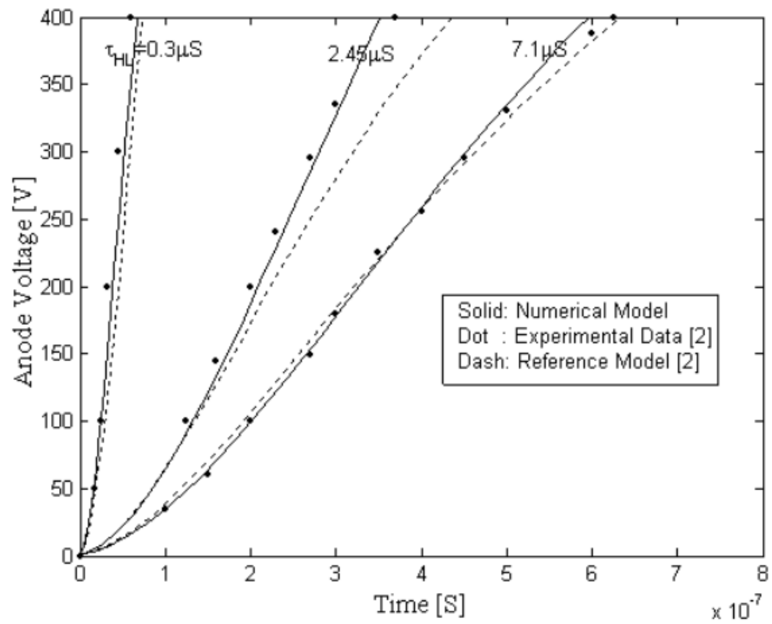

FIGURE 3.2: A comparison of the theoretical and measured 10A infinite inductive load switching voltage waveforms for devices with different base lifetimes [3]

Equation (3.8) is Hefner's transient $\frac{dV(t)}{dt}$model for IGBT and Q(t)is expressed by solving the following non-linear differential equation Parabolic by Hefner

$$\frac{dQ(t)}{dt} = \frac{-Q(t)}{\tau_{HL}} - \frac{4Q^2(t)Isne}{W^2(t)A^2q^2n_i^2} \qquad (3.9)$$

Where I_{sne} is emitter electron saturation current (A) and n_i is the intrinsic carrier concentration cm^{-3}.

In Hefner's [3] approach, the negative of the collected hole current $I_p(W(t))$ consists of a charged control current (I_{cc}) and redistribution current (I_p), which make this model more complex. The expression (3.9) is not simple and Q_0 cannot be easily determined since there is no expression for

P_0 Which can be substituted for in Q_0equation to evaluate $Q_0$for magnitude. Also, this model did not considerthe rate of change of C(t) in the calculation of the displacement current I_n(W(t)).

3.1.2 Redistribution time and Charge Control Current

Representative excess carrier distributions in the wide-base bipolar transient at various moments during a constant anode voltage turn-off transient are showing Fig. 3.3

When the base current is removed (constant anode voltage case) or the anode clamp voltage is reached (inductive load case), the carrier distribution in the base changes rapidly to one for which the total current at the emitter is equal to the hole current at the collector (from distribution (a) to (b) in Fig. 3.3), so that quasi-neutrality is maintained in the bipolar base. This reduction in the total device current is responsible for the initial rapid fall in current observed in the switching transient current waveform. The initial rapid fall consists principally of the steady-state net electron current at the collector (base current for the constant anode voltage case)and the component of hole drift current associated with the net electron current there. The remaining slowly decaying excess majority carrier store is responsible for the slowly decaying portion of the switching transient current wave form.

The boundary conditions on the electron and hole currents are different between the steady-state condition and the slowly decaying current phase. As a result, the electrons & holes that recombine can no longer be supplied be the divergence of their current densities as they are in steady-state, but are only supplied by (and thus reduce)the local excess carrier concentration. The curvature in the carrier distributions and the corresponding divergence of the current densities that remains after the initial rapid fall in emitter current acts to redistribute the excess carriers in the base from distribution (b) & (c) in Fig. 3.3.After the redistribution is complete, the excess carrier distribution and the terminal current are given in terms of the total excess carrier charge in the base, so the remainder of the waveform can be described using a charge control model. The redistribution time and the relation between the charge and current after the redistribution is complete are found from the time-dependent ambipolar diffusion equation with

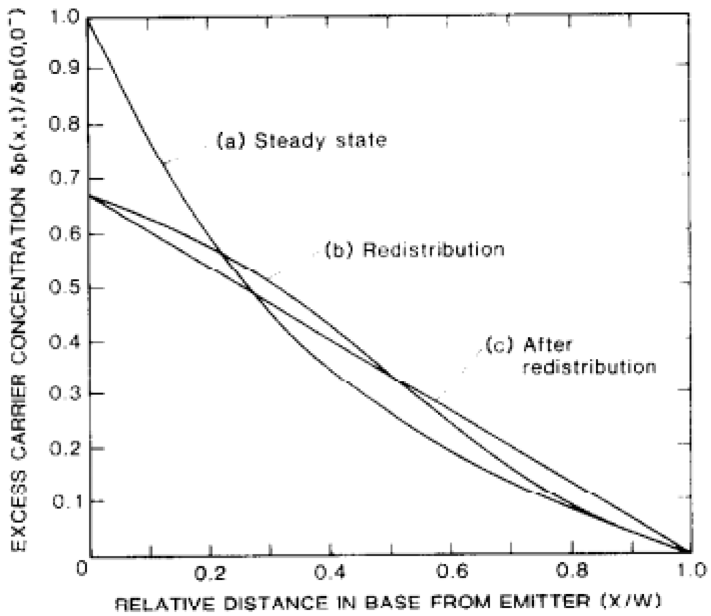

Figure 3.3: The Excess carrier distribution in the base before (a), during (b), and after (c) the redistribution phase of a constant anode voltage switching transient, for W/L=2.5 and for I_n(x= 0) <<I_p(x= 0). The effect of the decay of the total excess carrier has been left out to illustrate the redistribution process. [3]

I_n(W)=0 and the total current equal to emitter edge of the base for negligible electron current at the injected into the emitter to the collector current gives:

$$\frac{\partial P(x,t)}{\partial t} = \frac{\partial P(x,t)}{\partial t} \qquad (3.10)$$

The general solution to equation,

$$\frac{\partial^2 \delta p}{\partial x^2} = \frac{\partial p}{L^2} + \frac{1}{D}\frac{\partial \delta p}{\partial t}$$

With the conditions of:

$$\delta p(x = 0, t = 0) = P_0 \qquad (3.11)$$

$$\delta p(W, t) = 0 \qquad (3.12)$$

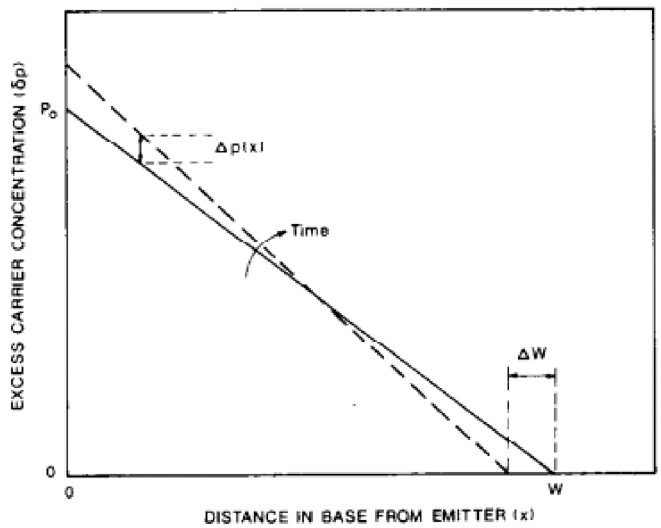

Figure 3.4: The carrier distribution in the base indicating the charge in excess carrier concentration with time due to the moving collector-base depletion edge boundary [3]

and equation (3.10) foe W independent of time is

$$\delta p(x,t) = P_{0,0}\left(1-\frac{x}{W}\right)e^{\left(\frac{-t}{\tau_{HL}}\right)} + \sum_{m=1}^{\infty} A_m \sin(2\pi m t) e^{\left(\frac{-t}{\tau m}\right)} \qquad (3.13)$$

Where

$$\frac{1}{\tau_m} = \frac{1}{\tau_{HL}} + \frac{(2m\pi)^2 D_p}{W^2} \qquad (3.14)$$

The first term of equation (3.13) is the linear charge control component of the distribution and the sine terms are the redistribution components which decay in time τ_m. For the base width W_B= 93× $10^{-6} m$ and other parameters,τ_m= $0.1/m^2 us$.For times much larger than this, the redistribution terms become negligible and the current is determined by linear charge control component of the distribution.

The redistribution terms are independent of the total base charge and the integrated charge of the charge control term is equal to the total excess base charge:

$$Q(t) = \frac{qAP_{0,0}W}{2} e^{\left(-\frac{t}{\tau_{HL}}\right)} \qquad (3.16)$$

Therefore, the current can only be described by a charge control model after there distribution is complete. Using equations (3.13) & (3.15) for I_n(W) = 0, the chargecontrol current is [Appendix A]

$$I_T(t) = \frac{4D_p}{W^2} Q(t) \tag{3.17}$$

Because the integrated charge of each of the redistribution terms is zero, the value of current obtained by extrapolating the current decay waveforms back to the time of the initial rapid fall in current corresponds to the value of current obtained from equation (3.16) evaluated for the initial charge.

Hefner assumed the depletion capacitance ($C_{bcj}(t)$) to be constant throughout
the whole process. But in reality, the depletion capacitance ($C_{bcj}(t)$) is a function of base depletion width (W_{bcj} (t)) as because

$$C_{bcj}(t) = \frac{A\varepsilon_{Si}}{W_{bcj}\ (\mathrm{t})}$$

The depletion capacitance is inversely proportional to the depletion width. So when the depletion width increases, capacitance decreases as well as effective base width (W(t)). This was not included in Hefner's approach which is the main limitation of the model.

Chapter 4

Transient Analysis through Parabolic Approximation

The main foundation of the Parabolic model by Hefner was based on the assumption that effective base width must be much less than the carrier diffusion length (W << L). But in case of base width greater than or equal to the diffusion length, the Parabolic models would give much variation than the experimental result. We have taken this limitation into account and have tried to propose a model that would give consistent result in all cases (W > L; W = L and W < L).

4.1 Approximation of Minority Carrier Concentration

In case of linear approximation, assuming,

$$\mathrm{W} < L$$

$$p(x,t) = P_0 \frac{\sin h\left(\frac{W-x}{L}\right)}{\sin h\left(\frac{W}{L}\right)}$$

turns to

$$p(x,t) = P_0 \left(1 - \frac{x}{L}\right) \tag{4.1}$$

But when

$$\mathrm{W} = L$$

Or

$$\mathrm{W} > L$$

is assumed, the two curves show large deviation.

According to parabolic approximation,

$$\sin h\left(\frac{W-x}{L}\right) = \frac{W-x}{L} + \frac{1}{6}\left(\frac{W-x}{L}\right)^3$$

$$\sin h\left(\frac{W}{L}\right) = \frac{W}{L} + \frac{1}{6}\left(\frac{W}{L}\right)^3$$

For carrier concentration

$$\text{p(x.t)} = P_0 \frac{\frac{W(t)-x}{L}+\frac{1}{6}\left(\frac{W(t)-x}{L}\right)^3}{\frac{W(t)}{L}+\frac{1}{6}\left(\frac{W(t)}{L}\right)^3} \tag{4.2}$$

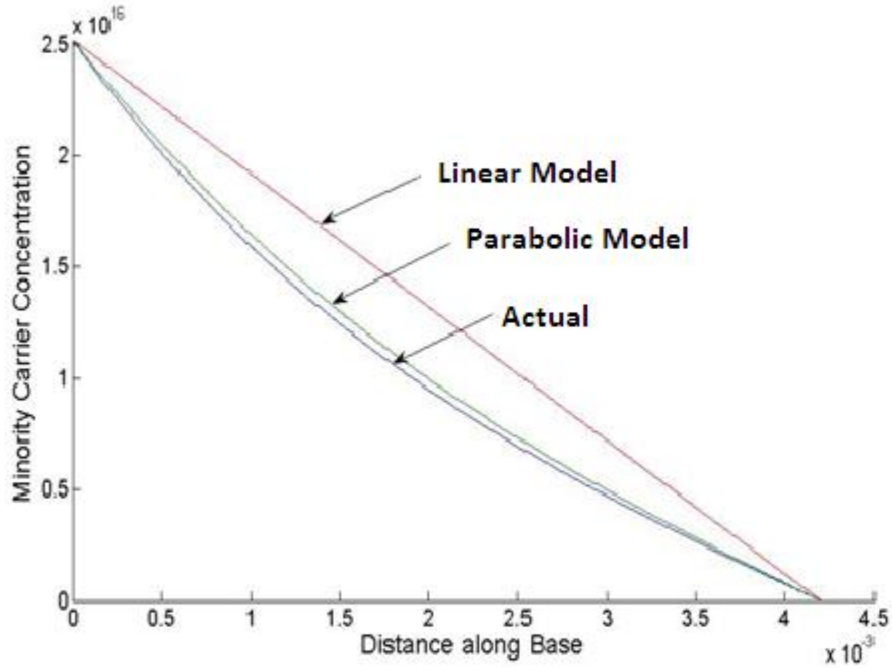

Figure 4.1: The carrier distribution in the base indicating the change in excess carrier concentration with distance in base for (W > L) (MATLAB)

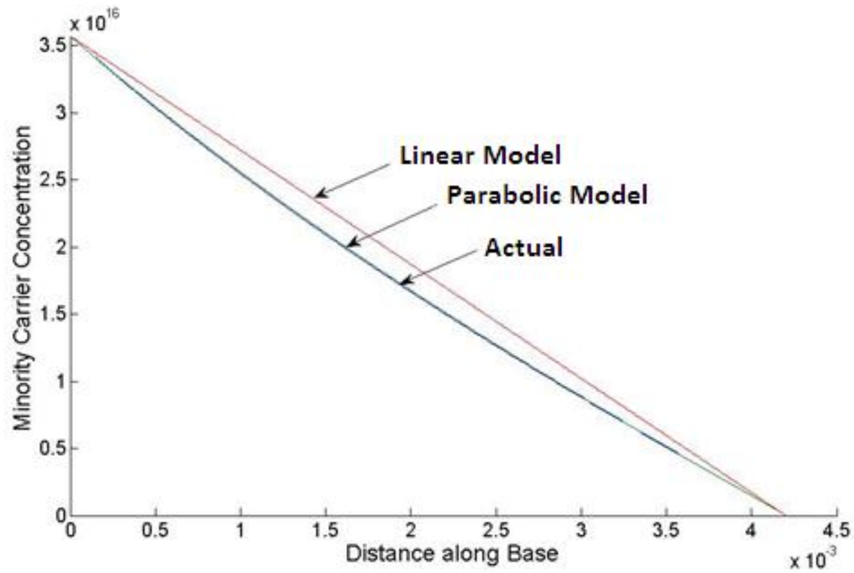

Figure 4.2: The carrier distribution in the base indicating the change in excess carrier concentration with distance in base for (W = L) (MATLAB).

which closely corresponds to the sinh curve for all values of W, unlike the linear approximation.

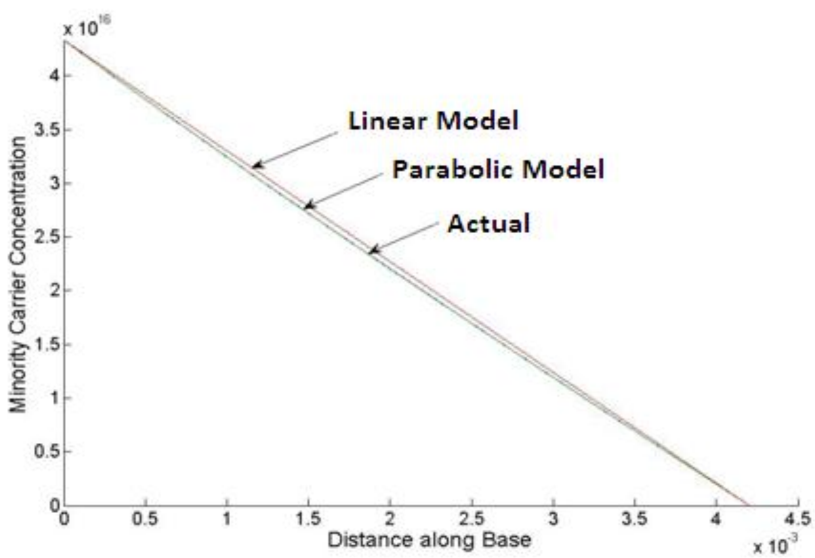

Figure 4.3: The carrier distribution in the base indicating the change in excess carrier concentration with distance in base for (W < L) (MATLAB).

$$p(x) = P_0 \frac{\frac{W-x}{L}+\frac{1}{6}\left(\frac{W-x}{L}\right)^3}{\frac{W}{L}+\frac{1}{6}\left(\frac{W}{L}\right)^3}$$

$$=P_0 \frac{\frac{6(W-x)L^2+(W-x)^3}{L^3}}{\frac{6WL^2+W^3}{L^3}}$$

$$=P_0 \frac{(W-x)[6L^2+(W-x)^2]}{W(6L^2+W^2)}$$

$$=P_0 \left(1-\frac{x}{W}\right)\frac{[6L^2+(W-x)^2]}{6L^2+W^2}$$

$$=P_0 \left[\frac{1+\frac{1}{6}\left(\frac{W-x}{L}\right)^2}{1+\frac{1}{6}\left(\frac{W}{L}\right)^2}\right]$$

So we have,

$$p(x,t) = P_0 \left[\frac{1+\frac{1}{6}(W(t)-x)^2}{1+\frac{1}{6}\left(\frac{W(t)}{L}\right)^2}\right] \quad (4.3)$$

In linear approximation, the charge was found to be

$$Q_0 = qAP_o \frac{W}{2} \quad (4.4)$$

and the actual value was

$$Q_0 = qAP_o L \tan h\left(\frac{W}{2L}\right) \quad (4.5)$$

Taking the parabolic approximation,

$$\tan h\left(\frac{W}{2L}\right) = \frac{W}{2L} - \frac{1}{3}\left(\frac{W}{2L}\right)^3$$

So, we take steady state excess base charge as

$$Q_0 = qAP_o L\left[\frac{W}{2L} - \frac{1}{3}\left(\frac{W}{2L}\right)^3\right]$$

$$= qAP_o L\left[\frac{W}{2L} - \frac{W^3}{24L^3}\right]$$

$$= qAP_o \left[\frac{W}{2} - \frac{W^3}{24L^2}\right]$$

So, $$P_0 = \frac{Q_0}{qA\left[\frac{W}{2} - \frac{W^3}{24L^2}\right]} \tag{4.6}$$

Now,

$$\frac{\partial P_0}{\partial t} = \frac{Q_0}{qA}(-1)\left[\frac{1}{2}\frac{\partial W}{\partial t} - \frac{1}{24L^2}3W^2\frac{\partial W}{\partial t}\right]$$

$$= -\frac{P_0}{\left[\frac{W}{2} - \frac{W^3}{24L^2}\right]}\left[\frac{1}{2} - \frac{1}{8L^2}W^2\right]\frac{\partial W}{\partial t}$$

$$= -\frac{P_0}{W}\frac{24L^2}{(12L^2 - W^2)}\left[\frac{1}{2} - \frac{W^2}{8L^2}\right]\frac{\partial W}{\partial t} \tag{4.7}$$

Now if we assume

$$W << L$$

$$\frac{\partial P_0}{\partial t} = -\frac{P_0}{W}\frac{24L^2}{12L^2}\frac{1}{2}\frac{\partial W}{\partial t}$$

$$\frac{\partial P_0}{\partial t} = -\frac{P_0}{W}\frac{\partial W}{\partial t} \tag{4.8}$$

This is the deduced expression by Hefner.

4.1.1 Ambipolar Diffusion Equation

$$\frac{\partial^2 p(x,t)}{\partial x^2} = \frac{p(x,t)}{L^2} + \frac{1}{D}\frac{\partial p(x,t)}{\partial t} \tag{4.9}$$

Integrating once,

$$\frac{\partial p(x,t)}{\partial x} = \frac{1}{L^2}\int p(x,t)\partial x + \frac{1}{D}\int \frac{\partial p(x,t)}{\partial t}\partial x \tag{4.10}$$

Again integrating equation (4.10), we get

$$p(x,t) = -\frac{P_0}{4WL^2(6L^2+W^2)}\left[12L^2\frac{(W-x)^3}{-3} + \frac{(W-x)^5}{-5}\right]$$
$$+\frac{1}{D}\frac{P_0}{W}\frac{\partial W}{\partial t}\frac{1}{4W(6L^2+W^2)}\frac{(12L^2-3W^2)}{(12L^2-W^2)}\left[12L^2\frac{(W-x)^3}{-3} + \frac{(W-x)^5}{-5}\right]$$
$$+\frac{1}{D}P_0\frac{1}{W^2(6L^2+W^2)}\frac{\partial W}{\partial t}\left[\frac{x^3}{6}(6L^2+W^2) - 2W\frac{x^4}{12} + \frac{x^5}{20}\right]$$

$$+\frac{1}{D}\frac{2P_0}{W(6L^2+W^2)}\frac{\partial W}{\partial t}\left[W(W^2-6L^2)\frac{x^3}{6}-(2W^2-6L^2)\frac{x^4}{12}+W\frac{x^5}{20}\right]+C_1x+C_2 \quad (4.11)$$

This is the expression for excess carrier concentration which is a function of x and t.

Boundary conditions:

$$x=0, p=p_0 \quad (4.12)$$

$$x=W, p=0 \quad (4.13)$$

Now putting the boundary values from equation (4.12) and (4.13) in equation (4.11), we get

$$\begin{aligned}p(x,t) &= \frac{P_0}{4WL^2(6L^2+W^2)}\left[4L^2(W-x)^3+\frac{(W-x)^5}{5}\right]\\ &-\frac{1}{D}\frac{P_0}{W}\frac{\partial W}{\partial t}\frac{1}{4W(6L^2+W^2)}\frac{(12L^2-3W^2)}{(12L^2-W^2)}\left[4L^2(W-x)^3+\frac{(W-x)^5}{5}\right]\\ &+\frac{1}{D}P_0\frac{1}{W^2(6L^2+W^2)}\frac{\partial W}{\partial t}\left[\frac{x^3}{6}(6L^2+W^2)-W\frac{x^4}{6}+\frac{x^5}{20}\right]\\ &+\frac{1}{D}\frac{2P_0}{W(6L^2+W^2)}\frac{\partial W}{\partial t}\left[W(W^2-6L^2)\frac{x^3}{6}-(2W^2-6L^2)\frac{x^4}{12}+W\frac{x^5}{20}\right]\\ &-\frac{1}{D}\frac{P_0x}{5}\frac{\partial W}{\partial t}\frac{(20L^2+W^2)}{(6L^2+W^2)}\left[\frac{(6L^2-W^2)}{(12L^2-W^2)}\right]-\frac{1}{D}\frac{P_0xW^2}{(6L^2+W^2)^2}\frac{\partial W}{\partial t}\left[\frac{W^2-10L^2}{10}\right]\\ &-\frac{p_0x}{W}+\frac{P_0x(20L^2+W^2)}{20(6L^2+W^2)}\frac{W}{L^2}+p_0-\frac{P_0(20L^2+W^2)}{20(6L^2+W^2)}\left[\frac{W^2}{L^2}-\frac{1}{D}\frac{\partial W}{\partial t}\frac{(12L^2-3W^2)}{(12L^2-W^2)}.W\right] \quad (4.14)\end{aligned}$$

This is actual the excess carrier concentration $p(x,t)$for base n-drift region.

Now we know, the excess base charge can be calculated by the following equation

$$Q(t)=qA\int_0^W p(x)dx \quad (4.15)$$

Integrating the excess carrier concentration, we get

$$\int p(x,t)dx=\frac{P_0}{20WL^2(6L^2+W^2)}\left[\frac{20L^2(W-x)^4}{-4}-\frac{(W-x)^6}{6}\right]$$

$$-\frac{1}{D}\frac{P_0}{20W^2}\frac{\partial W}{\partial t}\frac{1}{(6L^2+W^2)}\frac{(12L^2-3W^2)}{(12L^2-W^2)}\left[\frac{20L^2(W-x)^4}{-4}-\frac{(W-x)^6}{6}\right]$$

$$+\frac{1}{D}P_0\frac{1}{W^2(6L^2+W^2)}\frac{\partial W}{\partial t}\left[\frac{x^4}{24}(6L^2+W^2)-W\frac{x^5}{30}+\frac{x^6}{120}\right]$$

$$+\frac{1}{D}\frac{2P_0}{W(6L^2+W^2)}\frac{\partial W}{\partial t}\left[W(W^2-6L^2)\frac{x^4}{24}-(W^2-3L^2)\frac{x^5}{30}+W\frac{x^6}{120}\right]$$

$$-\frac{1}{D}\frac{P_0}{5}\frac{\partial W}{\partial t}\frac{(20L^2+W^2)}{(6L^2+W^2)}\left[\frac{(6L^2-W^2)}{(12L^2-W^2)}\right]\frac{x^2}{2}-\frac{1}{D}\frac{P_0W^2}{(6L^2+W^2)^2}\frac{\partial W}{\partial t}\left[\frac{W^2-10L^2}{10}\right]\frac{x^2}{2}$$

$$-\frac{p_0}{W}\frac{x^2}{2}+\frac{P_0(20L^2+W^2)}{20(6L^2+W^2)}\frac{W}{L^2}\frac{x^2}{2}\quad+p_0x-\frac{P_0(20L^2+W^2)}{20(6L^2+W^2)}\left[\frac{W^2}{L^2}-\frac{1}{D}\frac{\partial W}{\partial t}\frac{(12L^2-3W^2)}{(12L^2-W^2)}.W\right]x \quad (4.16)$$

Now we putting $x = W$ (upper limit) and $x = 0$ (lower limit) in $\int p(x,t)dx$ and if we assume W is much much smaller than L (W << L)

$$\int_0^W Pdx = \frac{1}{D}\frac{P_0W^2}{24}\frac{\partial W}{\partial t}$$

$$-\frac{1}{D}\frac{P_0W^4}{120L^2}\frac{\partial W}{\partial t}-\frac{1}{D}\frac{P_0W^2}{6}\frac{\partial W}{\partial t}+\frac{1}{D}\frac{P_0W^4}{72L^2}\frac{\partial W}{\partial t}+P_0\frac{W}{2}+\frac{P_0W^3}{12L^2}$$

$$-\frac{P_0W^3}{6L^2}+\frac{1}{D}\frac{P_0W^2}{6L^2}\frac{\partial W}{\partial t}+\frac{P_0W^3}{24L^2}-\frac{1}{D}\frac{P_0W^2}{4}\frac{\partial W}{\partial t}$$

$$\int_0^W Pdx = P_0\frac{W}{2}-\frac{P_0W^3}{24L^2}-\frac{3}{8}\frac{1}{D}P_0W^2\frac{\partial W}{\partial t} \quad (4.17)$$

Now the excess base charge will be

$$Q(t) = qA\int_0^W Pdx$$

$$= qAP_0\frac{W}{2}-qA\frac{P_0W^3}{24L^2}-qA\frac{3P_0W^2}{8D}\frac{\partial W}{\partial t}$$

$$= qA\left[P_0\frac{W}{2}-\frac{P_0W^3}{24L^2}\right]-qA\frac{3P_0W^2}{8D}\frac{\partial W}{\partial t} \quad (4.18)$$

As we know,

L= $\sqrt{D\tau_{HL}}$

$L^2 = D\tau_{HL}$

So, $D = \frac{L^2}{\tau_{HL}}$

$$qA\frac{3P_0W^2}{8D}\frac{\partial W}{\partial t} = qA\frac{3}{8}\frac{L^2}{W^2}P_0\frac{\partial W}{\partial t}\tau_{HL} \approx 0$$

As, $\frac{W}{L} << 1$

$$Q(t) = qA\left[P_0\frac{W}{2} - \frac{P_0W^3}{24L^2}\right] \quad (4.19)$$

Assuming $\frac{W}{L} << 1, \frac{W^3}{L^2} \approx 0$

$$Q(t) = qA\frac{P_0W(t)}{2} \quad (4.20)$$

4.2 Expression for Transient Anode Voltage

According to Allen R.Hefner:

$$p(x,t) = P_0\left[1 - \frac{x}{W(t)}\right] - \frac{1}{W(t)}\frac{\partial W}{\partial t}\frac{P_0}{D}\left[\frac{x^2}{2} - \frac{W(t)x}{6} - \frac{x^3}{3W(t)}\right] \quad (4.21)$$

Our derived expression

$$\begin{aligned}
p(x,t) &= \frac{P_0}{4WL^2(6L^2+W^2)}\left[4L^2(W-x)^3 + \frac{(W-x)^5}{5}\right] \\
&- \frac{1}{D}\frac{P_0}{W}\frac{\partial W}{\partial t}\frac{1}{4W(6L^2+W^2)}\frac{(12L^2-3W^2)}{(12L^2-W^2)}\left[4L^2(W-x)^3 + \frac{(W-x)^5}{5}\right] \\
&+ \frac{1}{D}P_0\frac{1}{W^2(6L^2+W^2)}\frac{\partial W}{\partial t}\left[\frac{x^3}{6}(6L^2+W^2) - W\frac{x^4}{6} + \frac{x^5}{20}\right] \\
&+ \frac{1}{D}\frac{2P_0}{W(6L^2+W^2)^2}\frac{\partial W}{\partial t}\left[W(W^2-6L^2)\frac{x^3}{6} - (2W^2-6L^2)\frac{x^4}{12} + W\frac{x^5}{20}\right] \\
&- \frac{1}{D}\frac{P_0x}{5}\frac{\partial W}{\partial t}\frac{(20L^2+W^2)}{(6L^2+W^2)}\left[\frac{(6L^2-W^2)}{(12L^2-W^2)}\right] - \frac{1}{D}\frac{P_0xW^2}{(6L^2+W^2)^2}\frac{\partial W}{\partial t}\left[\frac{W^2-10L^2}{10}\right] \\
&- \frac{p_0x}{W} + \frac{P_0x(20L^2+W^2)}{20(6L^2+W^2)}\frac{W}{L^2} \quad + p_0 - \frac{P_0(20L^2+W^2)}{20(6L^2+W^2)}\left[\frac{W^2}{L^2} - \frac{1}{D}\frac{\partial W}{\partial t}\frac{(12L^2-3W^2)}{(12L^2-W^2)}.W\right]
\end{aligned} \quad (4.22)$$

$I_n(W)$ = Dis-placement current

It is created from discharge of Reverse Biased Collector Base Depletion Junction Capacitance $C_{bcj}\ (t)$

In his journal, Hefner assumed $C_{bcj}\ (t)$ to be constant all through time which is not correct. $C_{bcj}\ (t)$ Varies with depletion width $W_{bcj}\ (t)$, which is a function of time.

$$I_n(W) = \frac{d}{dt}\left(C_{bcj} V_{CE}\right)$$

$$I_n(W) = V_{CE}\frac{dC_{bcj}}{dt} + C_{bcj}\frac{dV_{CE}}{dt}$$

Now,

$$C_{bcj} = \frac{A\epsilon_{si}}{W_{bcj}}$$

Here,

$$W_{bcj} = \sqrt{\frac{\epsilon_{Si}V_{CE}}{qN_B}}$$

So,

$$C_{bcj} = A\,\epsilon_{si}\sqrt{\frac{qN_B}{2\epsilon_{si}V_{CE}}}$$

As we know

$$W = W_B - W_{bcj}$$

$$\frac{dW}{dt} = -\frac{dC_{bcj}}{dt} \tag{4.23}$$

where,

W_B =Total Base Width

W = Effective Base Width

W_{bcj} = Depletion Region Width

So we get

$$\frac{dW_{bcj}}{dt} = \frac{1}{2}\sqrt{\frac{qN_B}{2\epsilon_{si}V_{CE}}}\,\frac{2\epsilon_{si}}{qN_B}\,\frac{dV_{CE}}{dt}$$

$$= \sqrt{\frac{q\epsilon_{si}N_B}{2V_{CE}}}\,\frac{1}{qN_B}\,\frac{dV_{CE}}{dt}$$

$$= \frac{C_{bcj}}{qAN_B}\,\frac{dV_{CE}}{dt}$$

$$\frac{dW}{dt} = -\frac{C_{bcj}}{qAN_B}\,\frac{dV_{CE}}{dt} \qquad (4.24)$$

$$\frac{dC_{bcj}}{dt} = A\,\frac{d}{dt}\sqrt{\frac{q\epsilon_{si}N_B}{2V_{CE}}}$$

$$= -A\,\frac{1}{2}\,\frac{1}{\sqrt{\frac{q\epsilon_{si}N_B}{2V_{CE}}}}\,\frac{q\epsilon_{si}N_B}{2}\,\frac{1}{{V_{CE}}^2}\,\frac{dV_{CE}}{dt}$$

$$= -\frac{1}{2}\,\frac{A^2}{C_{bcj}}\,\frac{q\epsilon_{si}N_B}{2}\,\frac{1}{{V_{CE}}^2}\,\frac{dV_{CE}}{dt}$$

$$V_{CE}\,\frac{dC_{bcj}}{dt} = -\frac{1}{4}\,\frac{A^2}{C_{bcj}}\,\frac{q\epsilon_{si}N_B}{V_{CE}}\,\frac{dV_{CE}}{dt}$$

So the displacement current is

$$I_n(W) = -\frac{1}{4}\,\frac{A^2}{C_{bcj}}\,\frac{q\epsilon_{si}N_B}{V_{CE}}\,\frac{dV_{CE}}{dt} + C_{bcj}\,\frac{dV_{CE}}{dt}$$

$$= C_{bcj}\,\frac{dV_{CE}}{dt}\left[-\frac{1}{4}\,\frac{A^2}{{C_{bcj}}^2}\,\frac{q\epsilon_{si}N_B}{V_{CE}} + 1\right]$$

$$= C_{bcj}\,\frac{dV_{CE}}{dt}\left[-\frac{1}{4}\,\frac{2V_{CE}}{q\epsilon_{si}N_B}\,\frac{q\epsilon_{si}N_B}{V_{CE}} + 1\right]$$

$$= C_{bcj}\,\frac{dV_{CE}}{dt}\left[1 - \frac{1}{2}\right]$$

$$= \frac{1}{2}\,C_{bcj}\,\frac{dV_{CE}}{dt} \qquad (4.25)$$

Now, Displacement Current Equation with Transistor Current & Diffusion Current

$$I_n(W) = \frac{I_T}{1+\frac{1}{b}} + qAD\,\frac{\partial p(x,t)}{\partial x}_{[x=W(t)]}$$

Now,

From Our equation of $p(x,t)$,we get

$$\frac{\partial p(x,t)}{\partial t} = \frac{P_0}{20WL^2(6L^2+W^2)}[20L^2 3(W-x)^2(-1) + 5(W-x)^4(-1)]$$

$$-\frac{1}{D}\frac{P_0}{20W^2}\frac{\partial W}{\partial t}\frac{1}{(6L^2+W^2)}\frac{(12L^2-3W^2)}{(12L^2-W^2)}[20L^2 3(W-x)^2(-1) + 5(W-x)^4(-1)]$$
$$+\frac{1}{D}P_0\frac{1}{W^2(6L^2+W^2)}\frac{\partial W}{\partial t}\left[\frac{3x^2}{6}(6L^2+W^2) - W\frac{4x^3}{6} + \frac{5x^4}{20}\right]$$
$$+\frac{1}{D}\frac{2P_0}{W(6L^2+W^2)^2}\frac{\partial W}{\partial t}\left[W(W^2-6L^2)\frac{3x^2}{6} - (W^2-3L^2)\frac{4x^3}{6} + W\frac{5x^4}{20}\right]$$
$$-\frac{1}{D}\frac{P_0}{5}\frac{\partial W}{\partial t}\frac{(20L^2+W^2)}{(6L^2+W^2)}\left[\frac{(6L^2-W^2)}{(12L^2-W^2)}\right] - \frac{1}{D}\frac{P_0W^2}{(6L^2+W^2)^2}\frac{\partial W}{\partial t}\left[\frac{W^2-10L^2}{10}\right]$$
$$-\frac{p_0}{W} + \frac{P_0(20L^2+W^2)}{20(6L^2+W^2)}\frac{W}{L^2}$$

$$\frac{\partial p(x,t)}{\partial t} = \frac{P_0}{20WL^2(6L^2+W^2)}[20L^2 3(W-x)^2(-1) + 5(W-x)^4(-1)]$$

$$-\frac{1}{D}\frac{P_0}{20W^2}\frac{\partial W}{\partial t}\frac{1}{(6L^2+W^2)}\frac{(12L^2-3W^2)}{(12L^2-W^2)}[20L^2 3(W-x)^2(-1)$$
$$+ 5(W-x)^4(-1)]$$
$$+\frac{1}{D}P_0\frac{1}{W^2(6L^2+W^2)}\frac{\partial W}{\partial t}\left[\frac{3x^2}{6}(6L^2+W^2) - W\frac{4x^3}{6} + \frac{5x^4}{20}\right]$$
$$+\frac{1}{D}\frac{2P_0}{W(6L^2+W^2)^2}\frac{\partial W}{\partial t}\left[W(W^2-6L^2)\frac{3x^2}{6} - (W^2-3L^2)\frac{4x^3}{6} + W\frac{5x^4}{20}\right]$$
$$-\frac{1}{D}\frac{P_0}{5}\frac{\partial W}{\partial t}\frac{(20L^2+W^2)}{(6L^2+W^2)}\left[\frac{(6L^2-W^2)}{(12L^2-W^2)}\right] - \frac{1}{D}\frac{P_0W^2}{(6L^2+W^2)^2}\frac{\partial W}{\partial t}\left[\frac{W^2-10L^2}{10}\right]$$
$$-\frac{p_0}{W} + \frac{P_0(20L^2+W^2)}{20(6L^2+W^2)}\frac{W}{L^2}$$

$$\left.\frac{\partial p\,(x,t)}{\partial t}\right|_{x=W} = \frac{1}{D}\frac{P_0}{W^2(6L^2+W^2)}\frac{\partial W}{\partial t}\left[\frac{W^2}{2}(6L^2+W^2)-\frac{2W^4}{3}+\frac{W^4}{4}\right]$$

$$+\frac{1}{D}\frac{2P_0}{W(6L^2+W^2)^2}\frac{\partial W}{\partial t}\left[W(W^2-6L^2)\frac{w^2}{2}-(W^2-3L^2)\frac{2w^3}{3}+\frac{w^5}{4}\right]$$

$$-\frac{1}{D}\frac{P_0}{5}\frac{\partial W}{\partial t}\frac{(20L^2+W^2)}{(6L^2+W^2)}\left[\frac{(6L^2-W^2)}{(12L^2-W^2)}\right]-\frac{1}{D}\frac{P_0W^2}{(6L^2+W^2)^2}\frac{\partial W}{\partial t}\left[\frac{W^2-10L^2}{10}\right]$$

$$-\frac{p_0}{W}+\frac{P_0(20L^2+W^2)}{20(6L^2+W^2)}\frac{W}{L^2}$$

$$\left.\frac{\partial p\,(x,t)}{\partial t}\right|_{x=W} = \frac{1}{D}\frac{P_0}{(6L^2+W^2)}\frac{\partial W}{\partial t}\left[3L^2+\frac{W^2}{2}-\frac{5W^2}{12}\right]$$

$$+\frac{1}{D}\frac{P_0}{(6L^2+W^2)^2}\frac{\partial W}{\partial t}\left[W^4-6L^2W^2-\frac{4}{3}(W^2-3L^2)W^2+\frac{W^4}{2}\right]$$

$$-\frac{1}{D}\frac{P_0}{5}\frac{\partial W}{\partial t}\frac{(20L^2+W^2)}{(6L^2+W^2)}\left[\frac{(6L^2-W^2)}{(12L^2-W^2)}\right]-\frac{1}{D}\frac{P_0}{(6L^2+W^2)^2}\frac{\partial W}{\partial t}\left[\frac{W^4-10L^2W^2}{10}\right]$$

$$-\frac{p_0}{W}+\frac{P_0(20L^2+W^2)}{20(6L^2+W^2)}\frac{W}{L^2}$$

$$\left.\frac{\partial p\,(x,t)}{\partial t}\right|_{x=W} = \frac{1}{D}\frac{P_0}{(6L^2+W^2)}\frac{\partial W}{\partial t}\left[3L^2+\frac{W^2}{12}\right]$$

$$+\frac{1}{D}\frac{P_0}{(6L^2+W^2)^2}\frac{\partial W}{\partial t}\left[W^4-6L^2W^2-\frac{4}{3}W^4+4L^2W^2+\frac{W^4}{2}\right]$$

$$-\frac{1}{D}\frac{P_0}{5}\frac{\partial W}{\partial t}\frac{(20L^2+W^2)}{(6L^2+W^2)}\left[\frac{(6L^2-W^2)}{(12L^2-W^2)}\right]-\frac{1}{D}\frac{P_0}{(6L^2+W^2)^2}\frac{\partial W}{\partial t}\left[\frac{W^4-10L^2W^2}{10}\right]$$

$$-\frac{p_0}{W}+\frac{P_0(20L^2+W^2)}{20(6L^2+W^2)}\frac{W}{L^2}$$

$$\left.\frac{\partial p\,(x,t)}{\partial t}\right|_{x=W} = \frac{1}{D}\frac{P_0}{(6L^2+W^2)}\frac{\partial W}{\partial t}\left[3L^2+\frac{W^2}{12}\right]+\frac{1}{D}\frac{P_0}{(6L^2+W^2)^2}\frac{\partial W}{\partial t}\left[\frac{1}{6}W^4-2L^2W^2\right]$$

$$-\frac{1}{D}\frac{P_0}{5}\frac{\partial W}{\partial t}\frac{(20L^2+W^2)}{(6L^2+W^2)}\left[\frac{(6L^2-W^2)}{(12L^2-W^2)}\right]-\frac{1}{D}\frac{P_0}{(6L^2+W^2)^2}\frac{\partial W}{\partial t}\left[\frac{W^4-10L^2W^2}{10}\right]$$

$$-\frac{p_0}{W}+\frac{P_0(20L^2+W^2)}{20(6L^2+W^2)}\frac{W}{L^2}$$

We know from parabolic approximation, the excess carrier concentration at $x = 0$ would be

$$P_0 = \frac{Q}{qA\left[\frac{W}{2}-\frac{W^3}{24L^2}\right]}$$

So,

$$qAD\,\frac{\partial p\,(x,t)}{\partial t}_{x=W} = qA\,\frac{P_0}{(6L^2+W^2)}\frac{\partial W}{\partial t}\left[3L^2+\frac{W^2}{12}\right] + qA\,\frac{P_0}{(6L^2+W^2)^2}\frac{\partial W}{\partial t}\left[\frac{1}{6}W^4-2L^2W^2\right]$$

$$-\,\mathrm{qA}\,\frac{P_0}{5}\frac{\partial W}{\partial t}\frac{(20L^2+W^2)}{(6L^2+W^2)}\left[\frac{(6L^2-W^2)}{(12L^2-W^2)}\right] - qA\,\frac{P_0}{(6L^2+W^2)^2}\frac{\partial W}{\partial t}\left[\frac{W^4-10L^2W^2}{10}\right]$$

$$-qADp_0\left[\frac{1}{W}-\frac{1}{20}\frac{W}{L^2}\frac{(20L^2+W^2)}{(6L^2+W^2)}\right]$$

$$qAD\,\frac{\partial p\,(x,t)}{\partial t}_{x=W} = qA\,\frac{Q}{qA\left[\frac{W}{2}-\frac{W^3}{24L^2}\right]}\left(-\frac{C_{bcj}}{qAN_B}\frac{dV_{CE}}{dt}\right)\left[\frac{3L^2+\frac{W^2}{12}}{(6L^2+W^2)}\right]$$

$$+qA\,\frac{Q}{qA\left[\frac{W}{2}-\frac{W^3}{24L^2}\right]}\left(-\frac{C_{bcj}}{qAN_B}\frac{dV_{CE}}{dt}\right)\left[\frac{\frac{1}{6}W^4-2L^2W^2}{(6L^2+W^2)^2}\right]$$

$$-\,\mathrm{qA}\,\frac{Q}{qA\left[\frac{W}{2}-\frac{W^3}{24L^2}\right]}\left(-\frac{C_{bcj}}{qAN_B}\frac{dV_{CE}}{dt}\right)\frac{(20L^2+W^2)}{(6L^2+W^2)}\left[\frac{(6L^2-W^2)}{(12L^2-W^2)}\right]$$

$$-qA\,\frac{Q}{qA\left[\frac{W}{2}-\frac{W^3}{24L^2}\right]}\left(-\frac{C_{bcj}}{qAN_B}\frac{dV_{CE}}{dt}\right)\frac{1}{(6L^2+W^2)^2}\left[\frac{W^4-10L^2W^2}{10}\right]$$

$$-qAD\,\frac{Q}{qA\left[\frac{W}{2}-\frac{W^3}{24L^2}\right]}\left[\frac{1}{W}-\frac{1}{20}\frac{W}{L^2}\frac{(20L^2+W^2)}{(6L^2+W^2)}\right]$$

$$qAD\,\frac{\partial p\,(x,t)}{\partial t}_{x=W} = \frac{Q}{\left[\frac{W}{2}-\frac{W^3}{24L^2}\right]}\left(-\frac{C_{bcj}}{qAN_B}\frac{dV_{CE}}{dt}\right)\left[\frac{3L^2+\frac{W^2}{12}}{(6L^2+W^2)}-\frac{1}{5}\frac{(20L^2+W^2)}{(6L^2+W^2)}\frac{(6L^2-W^2)}{(12L^2-W^2)}\right]$$

$$-\frac{Q}{\left[\frac{W}{2}-\frac{W^3}{24L^2}\right]}\left(-\frac{C_{bcj}}{qAN_B}\frac{dV_{CE}}{dt}\right)\frac{1}{(6L^2+W^2)^2}\left[\frac{1}{6}W^4-2L^2W^2\,\frac{W^4-10L^2W^2}{10}\right]$$

$$-D\,\frac{Q}{\left[\frac{W}{2}-\frac{W^3}{24L^2}\right]}\left[\frac{1}{W}-\frac{1}{20}\frac{W}{L^2}\frac{(20L^2+W^2)}{(6L^2+W^2)}\right]$$

As we know, the displacement current

$$I_n(W) = \frac{I_T}{1+\frac{1}{b}} + qAD \frac{\partial p(x,t)}{\partial x}_{[x=W(t)]}$$

$$\frac{1}{2} C_{bcj} \frac{dV_{CE}}{dt} = \frac{I_T}{1+\frac{1}{b}} + \frac{Q}{\left[\frac{W}{2} - \frac{W^3}{24L^2}\right]} \left(-\frac{C_{bcj}}{qAN_B} \frac{dV_{CE}}{dt}\right)$$

$$\left[\frac{3L^2+\frac{W^2}{12}}{(6L^2+W^2)} - \frac{1}{5} \frac{(20L^2+W^2)}{(6L^2+W^2)} \frac{(6L^2-W^2)}{(12L^2-W^2)} + \frac{\frac{1}{6}W^4-2L^2W^2}{(6L^2+W^2)^2} - \frac{\frac{W^4-10L^2W^2}{10}}{(6L^2+W^2)^2}\right]$$

$$-D \frac{Q}{\left[\frac{W}{2} - \frac{W^3}{24L^2}\right]} \left[\frac{1}{W} - \frac{1}{20} \frac{W}{L^2} \frac{(20L^2+W^2)}{(6L^2+W^2)}\right]$$

$$\frac{1}{2} C_{bcj} \frac{dV_{CE}}{dt} \left[1 + \frac{2Q}{qAN_B\left[\frac{W}{2} - \frac{W^3}{24L^2}\right]} \left(\frac{3L^2+\frac{W^2}{12}}{(6L^2+W^2)} - \frac{1}{5} \frac{(20L^2+W^2)}{(6L^2+W^2)} \frac{(6L^2-W^2)}{(12L^2-W^2)} + \frac{\frac{1}{15}W^4-L^2W^2}{(6L^2+W^2)^2}\right)\right]$$

$$= \frac{1}{1+\frac{1}{b}} \left[I_T(0) - D \frac{Q\left(1+\frac{1}{b}\right)}{\left[\frac{W}{2} - \frac{W^3}{24L^2}\right]} \left[\frac{1}{W} - \frac{1}{20} \frac{W}{L^2} \frac{(20L^2+W^2)}{(6L^2+W^2)}\right]\right]$$

$$\frac{dV_{CE}}{dt} = \frac{I_T(t) - \frac{2D_P Q(t)}{\left[\frac{W}{2} - \frac{W^3}{24L^2}\right]} \left[\frac{1}{W} - \frac{1}{20L^2} \frac{W(20L^2+W^2)}{(6L^2+W^2)}\right]}{\frac{1}{2} C_{bcj}\left(1+\frac{1}{b}\right)\left[1 + \frac{2Q(t)}{qAN_B\left[\frac{W}{2} - \frac{W^3}{24L^2}\right]}\left(\frac{3L^2+\frac{W^2}{12}}{(6L^2+W^2)} - \frac{1}{5}\frac{(20L^2+W^2)}{(6L^2+W^2)}\frac{(6L^2-W^2)}{(12L^2-W^2)} + \frac{\frac{1}{15}W^4-L^2W^2}{(6L^2+W^2)^2}\right)\right]} \tag{4.26}$$

This is the analytical expression for transient voltage of Non Punch IGBT.

Now if we assume,

$$W << L$$

$$\frac{W}{L} << 1$$

Then,

$$20L^2 + W^2 = 20L^2$$

$$6L^2 + W^2 = 6L^2$$

$$3L^2 + \frac{W^2}{12} = 3L^2$$

Now,

$$\frac{dV_{CE}}{dt} = \frac{I_T(t) - \frac{2D_P Q(t)}{\left[\frac{W}{2} - \frac{W^3}{24L^2}\right]}\left[\frac{1}{W} - \frac{1}{20L^2}\frac{W\,(20L^2+W^2)}{(6L^2+W^2)}\right]}{\frac{1}{2}C_{bcj}\left(1+\frac{1}{b}\right)\left[1+\frac{2Q(t)}{qAN_B\left[\frac{W}{2}-\frac{W^3}{24L^2}\right]}\left(\frac{3L^2+\frac{W^2}{12}}{(6L^2+W^2)} - \frac{1(20L^2+W^2)\,(6L^2-W^2)}{5\,(6L^2+W^2)\,(12L^2-W^2)} + \frac{\frac{1}{15}W^4 - L^2W^2}{(6L^2+W^2)^2}\right)\right]}$$

$$= \frac{I_T(t) - \frac{2D_P Q(t)}{\left[\frac{W}{2}\right]}\left[\frac{1}{W} - \frac{1}{20L^2}\frac{W\,(20L^2)}{(6L^2)}\right]}{\frac{1}{2}C_{bcj}\left(1+\frac{1}{b}\right)\left[1+\frac{2Q(t)}{qAN_B\left[\frac{W}{2}\right]}\left(\frac{3L^2}{6L^2} - \frac{1(20L^2)\,(6L^2)}{5\,(6L^2)\,(12L^2)} + \frac{\frac{1}{15}W^4 - L^2W^2}{36L^4}\right)\right]}$$

$$= \frac{I_T(t) - 4D_P\left[\frac{1}{W^2} - \frac{1}{6L^2}\right]Q(t)}{\frac{1}{2}C_{bcj}\left(1+\frac{1}{b}\right)\left[1+\frac{4Q(t)}{qAN_BW}\frac{1}{6}\right]}$$

$$\frac{dV_{CE}}{dt} = \frac{I_T(t) - 4D_P\left[\frac{1}{W^2} - \frac{1}{6L^2}\right]Q(t)}{\frac{1}{2}C_{bcj}\left(1+\frac{1}{b}\right)\left[1+\frac{2Q(t)}{3qAN_BW}\right]} \qquad (4.27)$$

Assuming,

$$W << L$$

$$\frac{1}{W^2} >> \frac{1}{6L^2}$$

So we neglect $\frac{1}{6L^2}$ terms find out

$$\frac{dV_{CE}}{dt} = \frac{I_T(t) - \frac{4D_P Q(t)}{W(t)^2}}{\frac{1}{2}C_{bcj}\left(1+\frac{1}{b}\right)\left[1+\frac{2Q(t)}{3qAN_BW}\right]} \qquad (4.28)$$

This is the expression for the transient voltage derived by Allen R. Hefner Jr & David L. Blackburn (1988) in the journal.

4.3 Expression for stored charge decay

We know due to the injection into the emitter, stored charge in the base would decay. The total charge decay rate would be

$$\frac{dQ(t)}{dt} = -\frac{Q(t)}{\tau_{HL}} - I_n(0)$$

Using the quasi-equilibrium simplification (i,e. the difference between the electron & hole quasi fermi potentials is the same on the both sides of the junction) and assuming high-level injection of the holes into the base, the electron current at the emitter-base junction $I_n(0)$ is related to $P_n(0)$ by :

$$\frac{I_n(0)}{I_{sne}} = e^{\frac{q}{kt}(\varphi_{pej} - \varphi_{nej})} = \frac{P_0(N_B + P_0)}{n_i^2} \approx \frac{P_0^2}{n_i^2}$$

Where,

φ_{nej} =Electron quasi fermi potential at E-B junction.

φ_{pej} =Hole quasi fermi potential at E-B junction.

I_{sne} =Emitter electron saturation current which accounts or the emitter parameters (Similar to the emitter Gummel Number).

The approximate form follows from the assumption that the basic is in high-level injection.

Now we assume

$$P_0 = \frac{Q}{qA\left[\frac{W}{2} - \frac{W^3}{24L^2}\right]}$$

$$I_n(0) = \frac{P_0^2}{n_i^2} I_{sne}$$

$$I_n(0) = \frac{Q^2}{q^2A^2\left[\frac{W}{2} - \frac{W^3}{24L^2}\right]^2} \frac{I_{sne}}{n_i^2}$$

$$\frac{dQ(t)}{dt} = -\frac{Q(t)}{\tau_{HL}} - \frac{Q^2}{q^2A^2\left[\frac{W}{2} - \frac{W^3}{24L^2}\right]^2} \frac{I_{sne}}{n_i^2} \qquad (4.29)$$

This is the expression for the stored charge decay rate

If

$$W << L$$

Then

$$\frac{W^3}{24L^2} \approx 0$$

So,

$$\frac{dQ(t)}{dt} \approx -\frac{Q(t)}{\tau_{HL}} - \frac{Q(t)^2}{q^2A^2\frac{W(t)^2}{4}} \frac{I_{sne}}{n_i^2}$$

$$\approx -\frac{Q(t)}{\tau_{HL}} - \frac{4Q(t)^2}{q^2A^2W(t)^2} \frac{I_{sne}}{n_i^2}$$

$$\frac{dQ(t)}{dt} \approx -\frac{Q(t)}{\tau_{HL}} - \frac{4Q(t)^2 I_{sne}}{q^2A^2[W_B - W_{bcj}(t)]^2 n_i^2} \quad (4.30)$$

Chapter 5

Results & Discussion

In this chapter, we compare parabolic models vs linear models for different carrier lifetimes. To do so, we perform some simulations on minority carrier concentration, anode voltage, anode current, base charge & last but not the least the switching power loss in MATLAB and the resulting graphs are prepared in Origin Pro 8 software.

5.1 Simulations for Minority Carrier Concentration:

A. case: High carrier Lifetime:

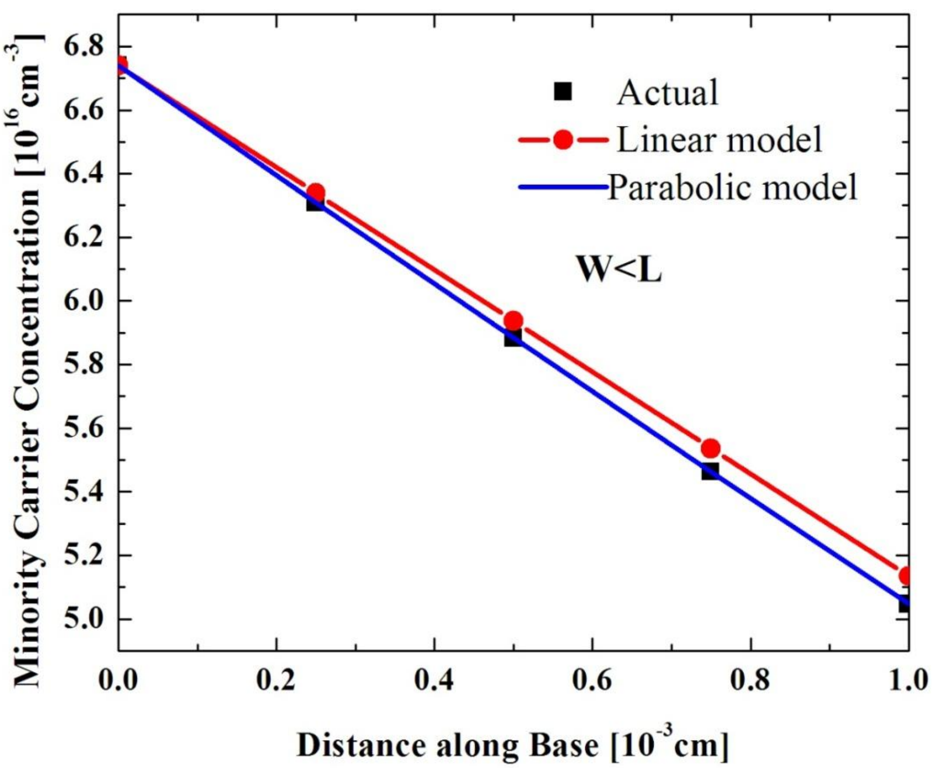

Figure-5.1.1: The carrier distribution in the base indicating the change in excess Carrier concentration with distance in base for (W < L)

In the figure, we compare the parabolic model and linear model with the actual model under the condition when the effective base width is lower than the diffusion length. Here, we can see for, the parabolic model is closer to actual model than the linear model. Moreover, it is also clear that, for τ_{HL} = 3.92 μs both the parabolic as well linear model show good agreement with the actual model. The main reason behind this incidence is the failure of recombination of large amount of charge before they reach to collector-base junction during transient turn-off. In this case, the effective base width is less than the diffusion length.

<u>B.case : Moderate carrier Lifetime:</u>

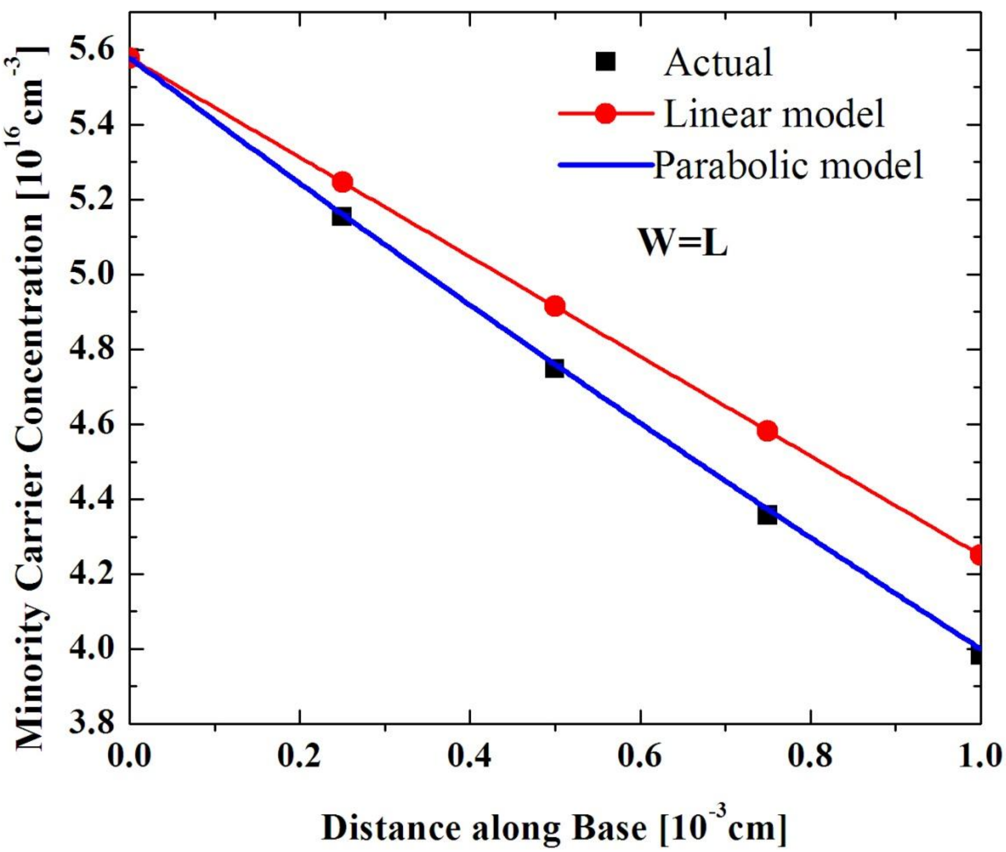

Figure-5.1.2: The carrier distribution in the base indicating the change in excess Carrier concentration with distance in base for (W = L)

In figure-5.1.2, we consider the diffusion length is equal to effective base width. In this case, for τ_{HL} = 1 µs, the linear model deviate a bit from the actual model, while the parabolic model shows a better agreement. Here the carrier life time is neither low nor high. As a result, a few number of charge carrier can reach to collector-base junction during turn off operation, which results significant recombination of the charge in the base region. However, the access carrier concentration cannot be linearly approximated. The parabolic model can justify the effect correctly, whereas the linear model fails to do that.

C.Case: Low carrier Lifetime:

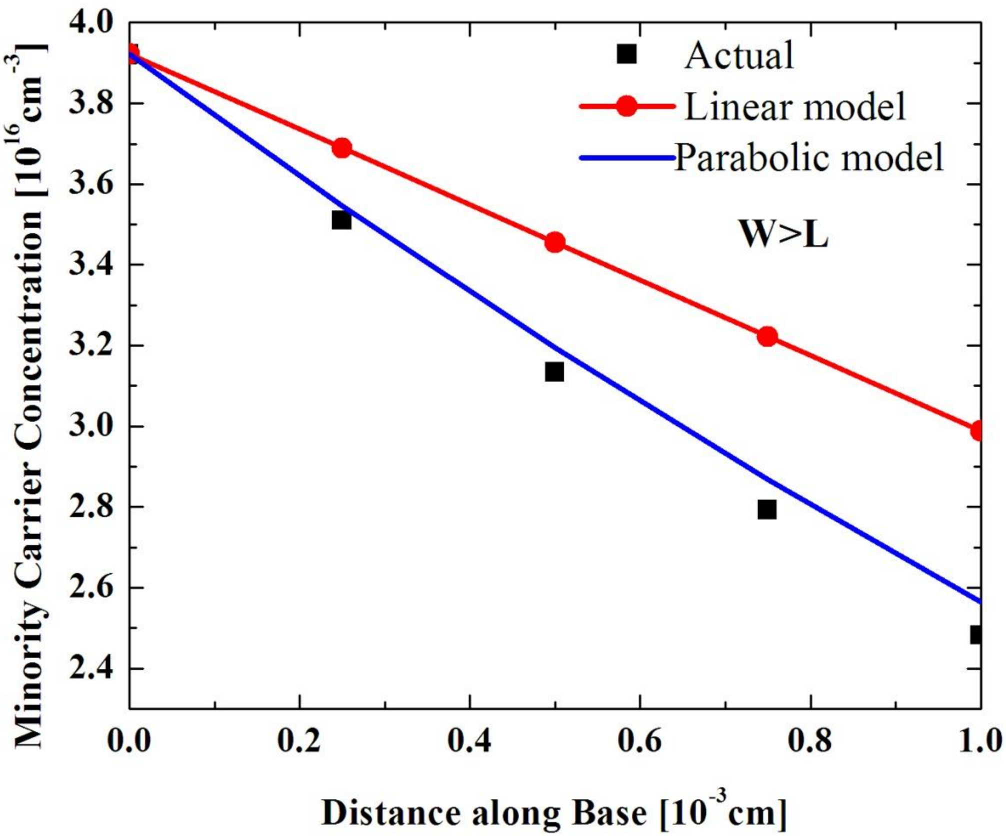

Figure-5.1.3: The carrier distribution in the base indicating the change in excess Carrier concentration with distance in base for (W > L)

Figure-5.1.3 represents a better consistency of parabolic model with the actual model for τ_{HL} = 0.32 μs whereas linear model shows greater deviation. Here the diffusion length is less than effective base width which result reverse biased condition of IGBT. In this case, as the carrier lifetime remains low, only a little amount of excess minority carrier can reach to the collector-base junction during transient turn-off. As a result high amount of recombination occurs. Once again, the parabolic model can predict the phenomenon correctly, whereas the linear model fails to do that.

Table 5.1.1 : Data analysis of Minority carrier concentration in different carrier lifetime

Carrier Lifetime (μs)	**Distance along the base (10^{-3}cm)**	**Minority carrier concentration(10^{16} cm^{-3})**				
		Actual	**Linear Model**	**Difference (%)**	**Parabolic**	**Difference (%)**
High (3.92)	0.00	6.74	6.74	0.00%	6.74	0.00%
	0.25	6.31	6.34	0.48%	6.31	0.01%
	0.5	5.88	5.94	0.92%	5.88	0.02%
	0.75	5.46	5.54	1.35%	5.46	0.03%
	1.00	5.05	5.13	1.74%	5.05	0.03%
Moderate (1)	0.00	5.58	5.58	0.00%	5.58	0.00%
	0.25	5.15	5.25	1.80%	5.16	0.14%
	0.50	4.75	4.91	3.52%	4.76	0.27%
	0.75	4.36	4.58	5.17%	4.37	0.37%
	1.00	3.98	4.25	6.74%	4.00	0.45%
Low (0.32)	0.00	3.92	3.92	0.00%	3.92	0.00%
	0.25	3.51	3.69	5.13%	3.54	1.03%
	0.50	3.13	3.46	10.28%	3.19	1.93%
	0.75	2.79	3.22	15.40%	2.87	2.71%
	1.00	2.48	2.99	20.45%	2.56	3.38%

5.2 Simulations for Charge:

A.case : High carrier Lifetime:

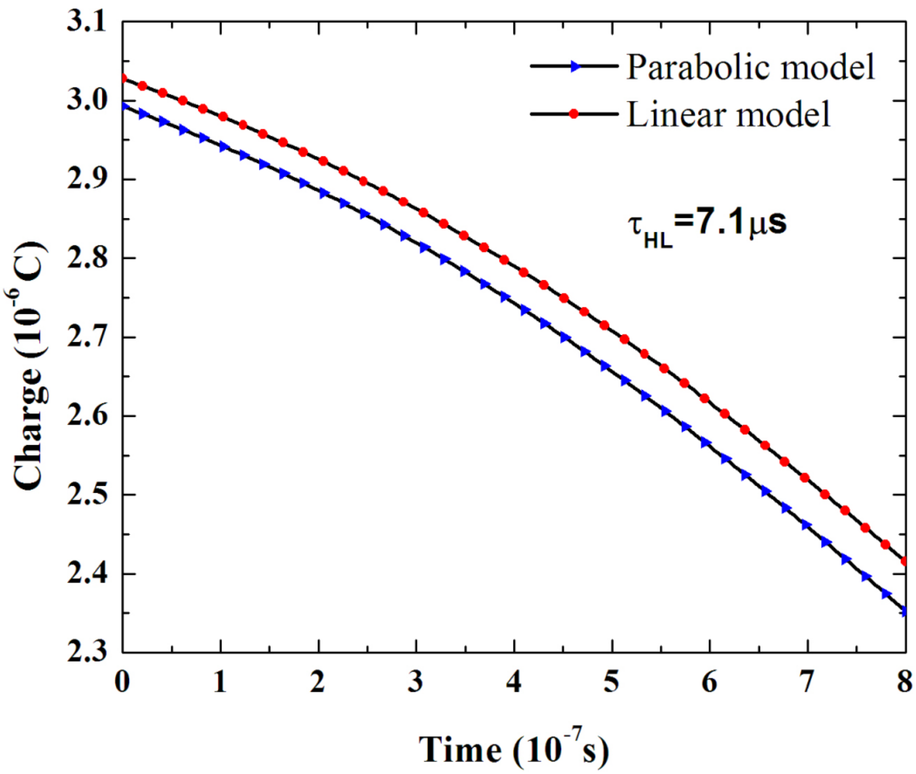

Figure 5.2.1: A comparison of theoretical (parabolic model and linear model) excess base charge for devices with different base lifetimes (τ_{HL} = 7.1 μs)

In case of τ_{HL} = 7.1 μs gives us indication that a large number of charge fail to recombine at this stage before they reach the collector-base junction. As a result the effective base width is smaller than the ambipolar diffusion length. So, huge charge builds up in the base region.

B.case: Moderate carrier Lifetime:

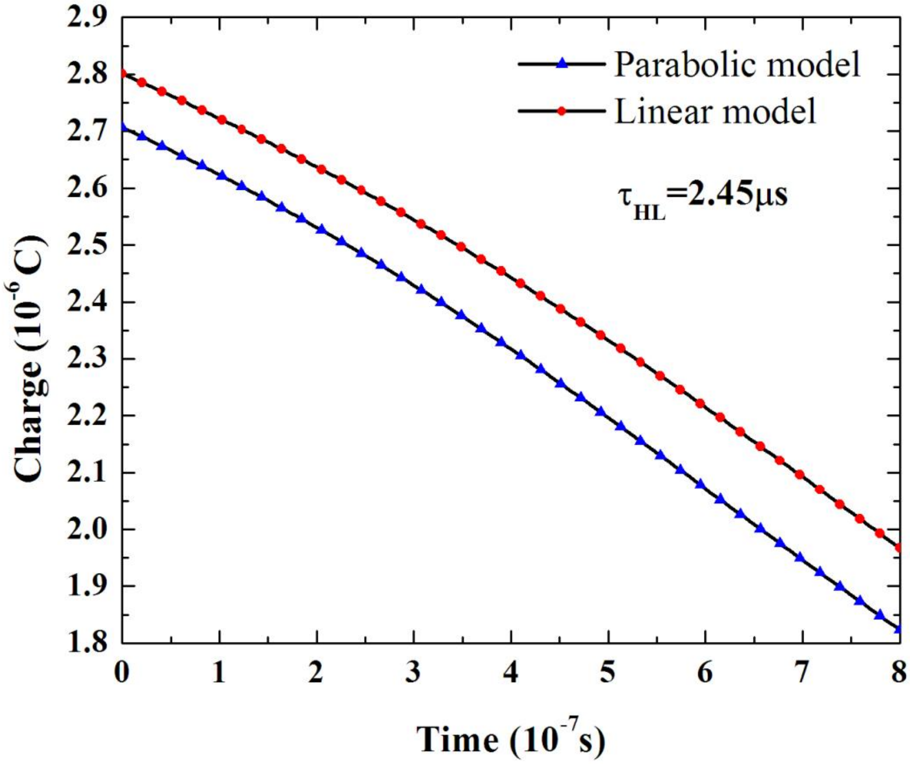

Figure 5.2.2: A comparison of theoretical (parabolic model and linear model) excess base charge for devices with different base lifetimes (τ_{HL} = 2.45 µs)

For, τ_{HL} = 2.45 µs in fig-5, parabolic model shows better consistency than linear model for moderate carrier life time. Here, carrier lifetime is neither high nor low and only some the charge carriers are able to reach the collector base junction before they recombine. In this case, the base width is equal to the ambipolar diffusion length which results in small charge build up in the base region.

C.case: Low carrier Lifetime:

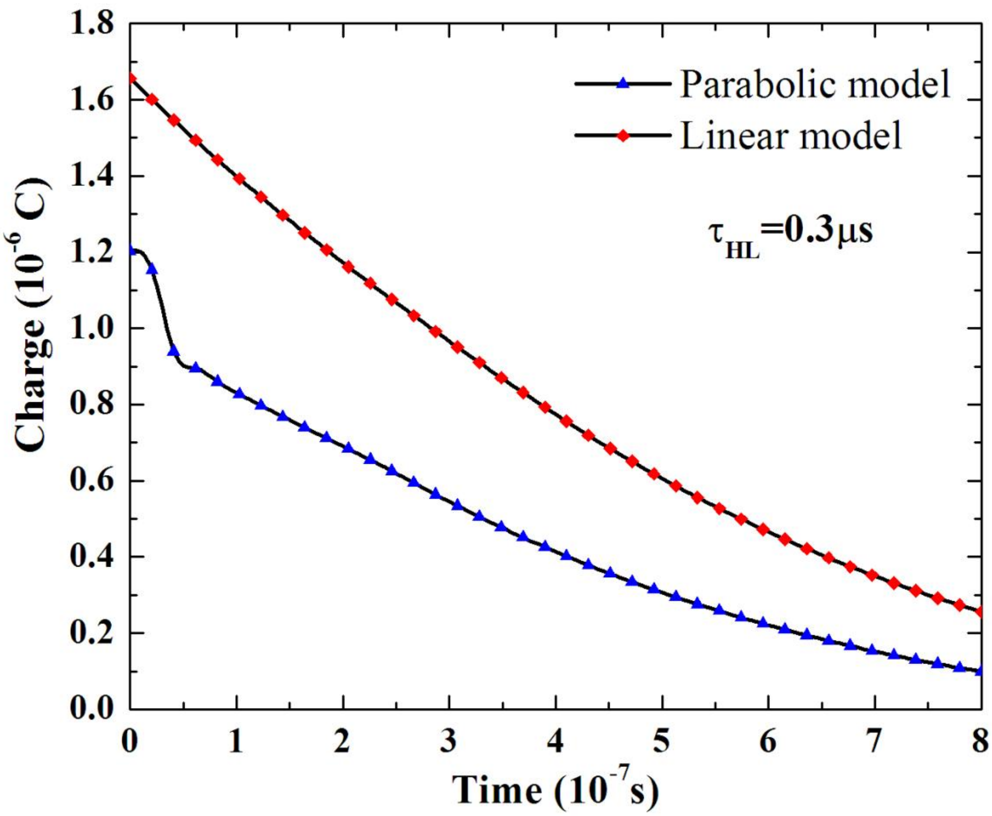

Figure 5.2.3: A comparison of theoretical (parabolic model and linear model) excess base charge for devices with different base lifetimes (τ_{HL} = 0.3 μs)

Fig-6 shows the case of low carrier lifetime, where τ_{HL} = 0.3 μs. In this case the base width is larger than the ambipolar diffusion length. The fact behind this phenomenon is that a small amount of excess minority carriers able to reach the collector-base junction before recombination which result a few charge to builds up in the base region.

Table 5.2.1: Data analysis of charge at different lifetime for parabolic & linear model

Carrier Lifetime (μs)	Time (10^{-7}s)	Charge (10^{-6} C)		
		Parabolic Model	Linear Model	Difference
High (7.1)	0.205	2.983	3.019	0.035
	1.026	2.942	2.979	0.037
	2.051	2.883	2.923	0.040
	3.077	2.814	2.857	0.043
	4.103	2.735	2.782	0.047
	5.128	2.645	2.697	0.052
	6.154	2.546	2.602	0.056
	7.179	2.441	2.501	0.060
	8.000	2.353	2.415	0.063
Moderate (2.45)	0.205	2.690	2.785	0.095
	1.026	2.621	2.720	0.099
	2.051	2.526	2.633	0.107
	3.077	2.421	2.537	0.116
	4.103	2.305	2.432	0.127
	5.128	2.181	2.318	0.137
	6.154	2.052	2.196	0.144
	7.179	1.924	2.070	0.146
	8.000	1.824	1.967	0.143
Low (0.3)	0.205	1.154	1.601	0.447
	1.026	0.828	1.393	0.566
	2.051	0.684	1.162	0.478
	3.077	0.534	0.951	0.417
	4.103	0.402	0.756	0.354
	5.128	0.295	0.587	0.292
	6.154	0.209	0.446	0.237
	7.179	0.142	0.332	0.190
	8.000	0.099	0.256	0.157

5.3 Simulations for Anode Voltage :

Output transient voltage characteristic depends on carrier life time as well as the drift region. If the drift region is higher than the diffusion region than the carrier life time will be lower. Lower carrier life time gives us the indication of transient output anode voltage rise will be faster during the turn off the IGBT compare to moderate and high carrier lifetime. After analyzing the curve for various carrier lifetime, we found that transient anode voltage rise is faster for the parabolic model compare to that of the linear model, which makes it better than linear model.

A.case: High carrier Lifetime:

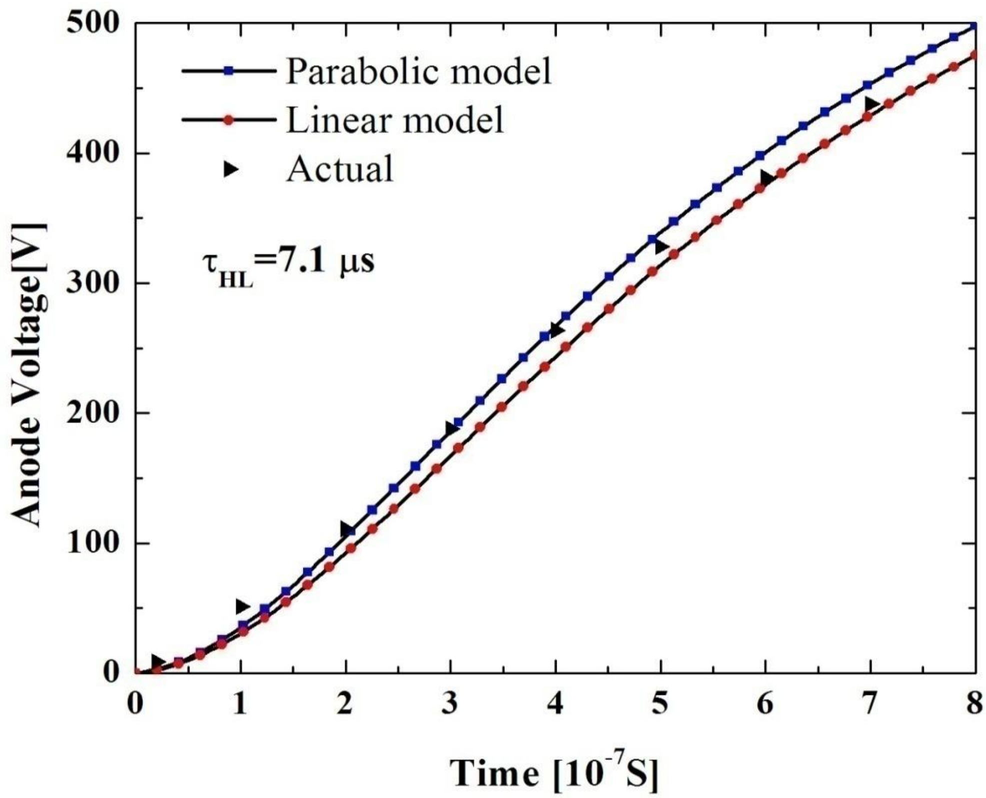

Figure-5.3.1: A comparison between parabolic model and linear model
for the transient switching anode voltage for different carrier lifetime(τ_{HL} = 7.1 µs)

In the Figure-7, τ_{HL} = 7.1 µs indicates a high carrier lifetime. When the carrier lifetime is high, large time is required to remove the minority carrier (hole) produced during on state of IGBT. Finally it makes the output anode voltage to rise slower than the moderate and lower carrier lifetime during turn-off. From the figure, it is clear that both the parabolic model as well as linear model show good consistency with the actual model.

B.case :Moderate carrier Lifetime:

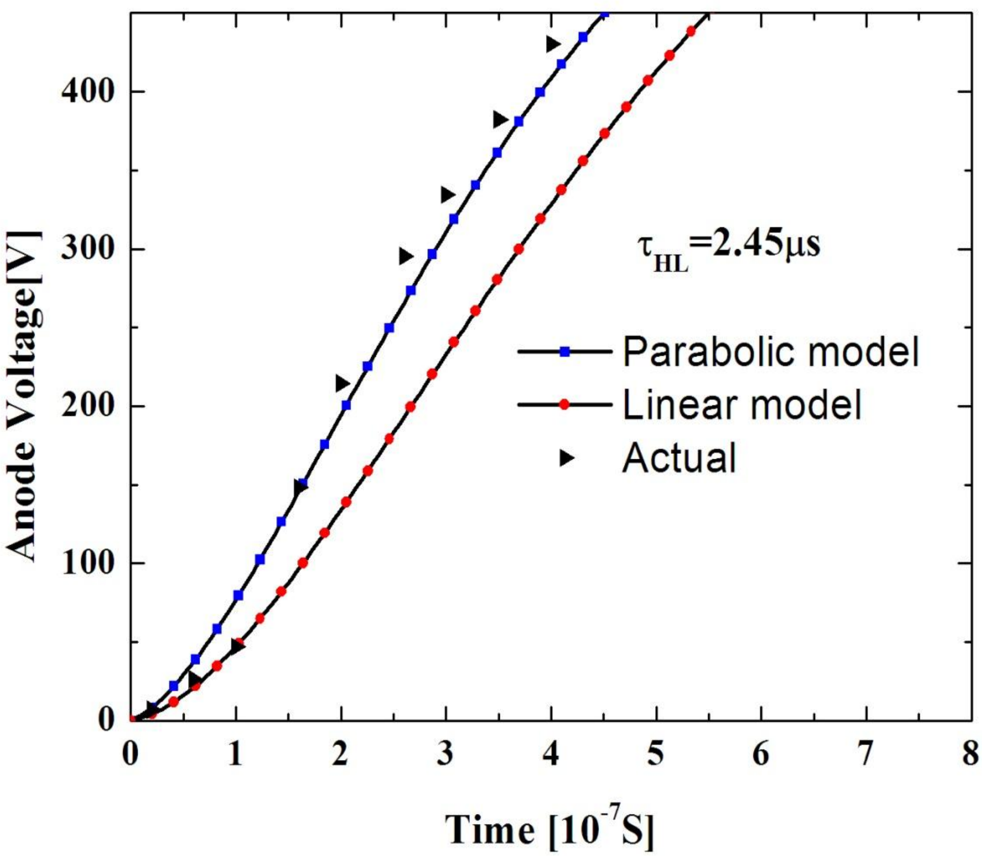

Figure 5.3.2: A comparison between parabolic model and linear model for the transient switching anode voltage for different carrier lifetime(τ_{HL} = 2.45 µs)

Figure 8 shows the moderate carrier life time which is τ_{HL} = 2.45 µs. From the figure it is showed that the voltage rise is faster compare to high carrier lifetime because it takes less time to remove excess minority carrier (hole) than that of the high carrier lifetime. In this situation, parabolic model has better accuracy than linear model. It also shows consistency in case of reverse blocking IGBT (RB-IGBT).

C.case : Low carrier Lifetime:

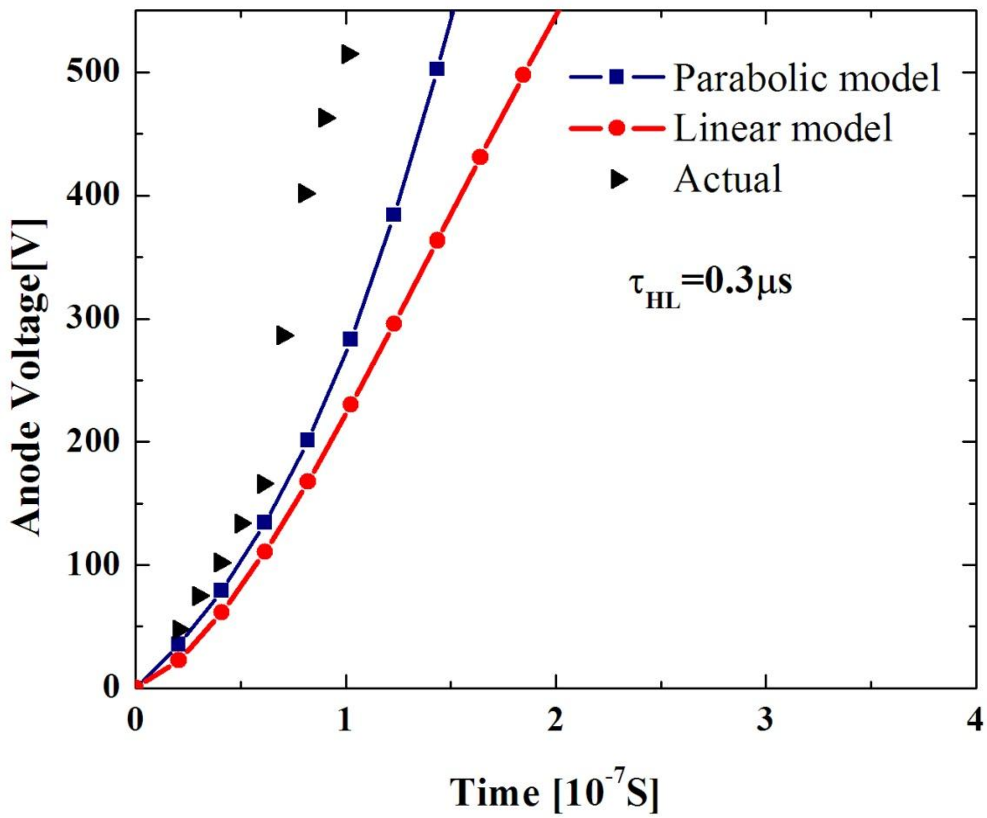

Figure-5.3.3: A comparison between parabolic model and linear model for the transient switching anode voltage for different carrier lifetime(τ_{HL} = 0.3 μs)

Figure 5.3.3 shows a low carrier lifetime that is τ_{HL} = 0.3 μs. In this case, at low carrier lifetime, output transient anode voltage rise rapidly compare to other conditions as a very few time is required for the removal of the excess minority carrier and to reach to the supply bus voltage (Vbus = 400 V) during the turn-off IGBT. Here, the parabolic model show much faster output voltage rise than linear model.

Table 5.3.1: Data analysis of Transient Anode Voltage at different carrier lifetime

Carrier Lifetime (μs)	**Time (10^{-7}s)**	**Anode Voltage (V)**				
		Actual Model	**Parabolic Model**	**Difference**	**Linear Model**	**Difference**
High (7.1)	0.2	8.659	3.059	64.67%	2.639	69.52%
	1.0	51.248	36.783	28.23%	31.709	38.13%
	2.0	111.023	109.078	1.75%	95.989	13.54%
	3.0	187.806	192.965	2.75%	173.229	7.76%
	4.0	263.716	274.567	4.11%	250.864	4.87%
	5.0	328.014	347.360	5.90%	322.171	1.78%
	6.0	381.304	409.521	7.40%	384.549	0.85%
	7.0	437.806	461.877	5.50%	437.995	0.04%
Moderate (2.45)	0.2	7.096	8.552	20.52%	4.428	37.60%
	0.6	26.423	38.893	47.19%	22.296	15.62%
	1.0	46.943	79.703	69.79%	49.091	4.58%
	1.6	148.390	150.883	1.68%	100.330	32.39%
	2.0	214.520	200.584	6.50%	138.942	35.23%
	2.6	295.610	273.421	7.51%	199.731	32.43%
	3.0	334.607	318.959	4.68%	240.506	28.12%
	3.5	382.431	361.181	5.56%	280.481	26.66%
	4.0	430.131	417.564	2.92%	337.664	21.50%
Low (0.3)	0.2	47.774	35.421	25.86%	22.580	52.74%
	0.3	74.939	54.866	26.79%	40.146	46.43%
	0.4	102.058	79.157	22.44%	61.453	39.79%
	0.5	133.820	103.041	23.00%	81.630	39.00%
	0.6	166.138	134.370	19.12%	110.843	33.28%
	0.7	286.375	160.584	43.93%	135.158	52.80%
	0.8	401.717	200.981	49.97%	167.817	58.23%
	0.9	463.017	234.185	49.42%	194.039	58.09%
	1.0	514.937	283.127	45.02%	230.144	55.31%

5.4 Simulations for Anode Current:

Anode current also depends the carrier lifetime like anode voltage. It has a proportional relationship with the carrier lifetime. If the carrier lifetime is high, the rise of carrier anode voltage will be slower compare to moderate and lower carrier lifetime during the turn-off. As a result, current decay slowly which gives us the indication of high anode current. In this case the parabolic model is better than the linear model as less current flows in parabolic model compare to linear model.

A.case :High carrier Lifetime:

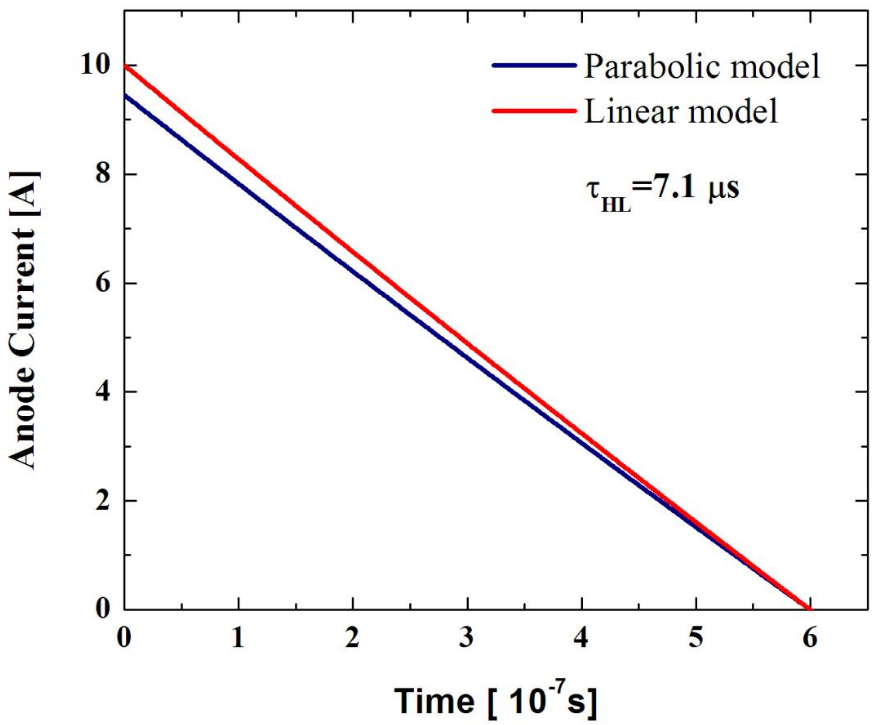

Figure-5.4.1: A comparison between parabolic model and linear model for the anode current for different carrier lifetime(τ_{HL} = 7.1 µs)

Figure-5.4.1 shows a high carrier lifetime τ_{HL} = 7.1µs. In this case, the anode current decay is slower than moderate and low carrier lifetime. A high carrier lifetime requires more time for extraction when the device turns off. As the transient anode current is higher than the other condition, the power loss is much larger. Here, less current is flowing through parabolic model at the same time.

B.case: Moderate carrier Lifetime:

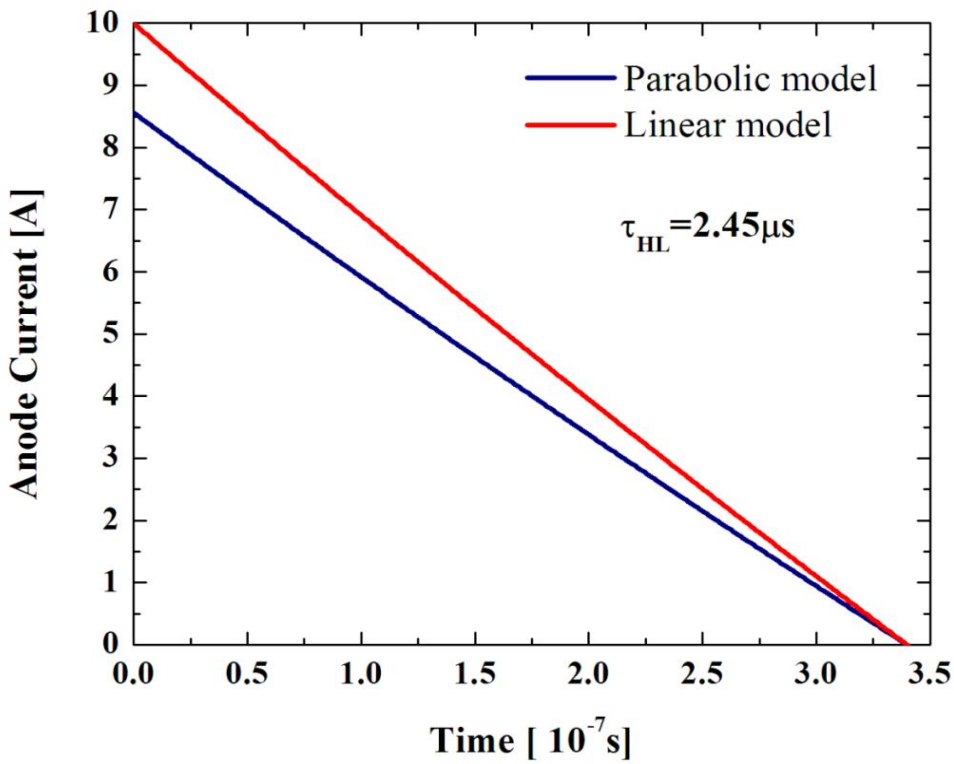

Figure-5.4.2: A comparison between parabolic model and linear model for the anode current for different carrier lifetime(τ_{HL} = 2.45 μs)

Figure-5.4.2 shows a moderate carrier lifetime which is τ_{HL} = 2.45 μs. In moderate carrier lifetime anode current decay is faster than the high carrier lifetime. Also a moderate carrier lifetime requires less time for removal of minority carrier (hole) when the device turns off. As a result the voltage rises faster than high carrier lifetime. So, power loss will decrease a bit. The parabolic model shows a faster decay of transient anode current.

C.case: Low carrier Lifetime:

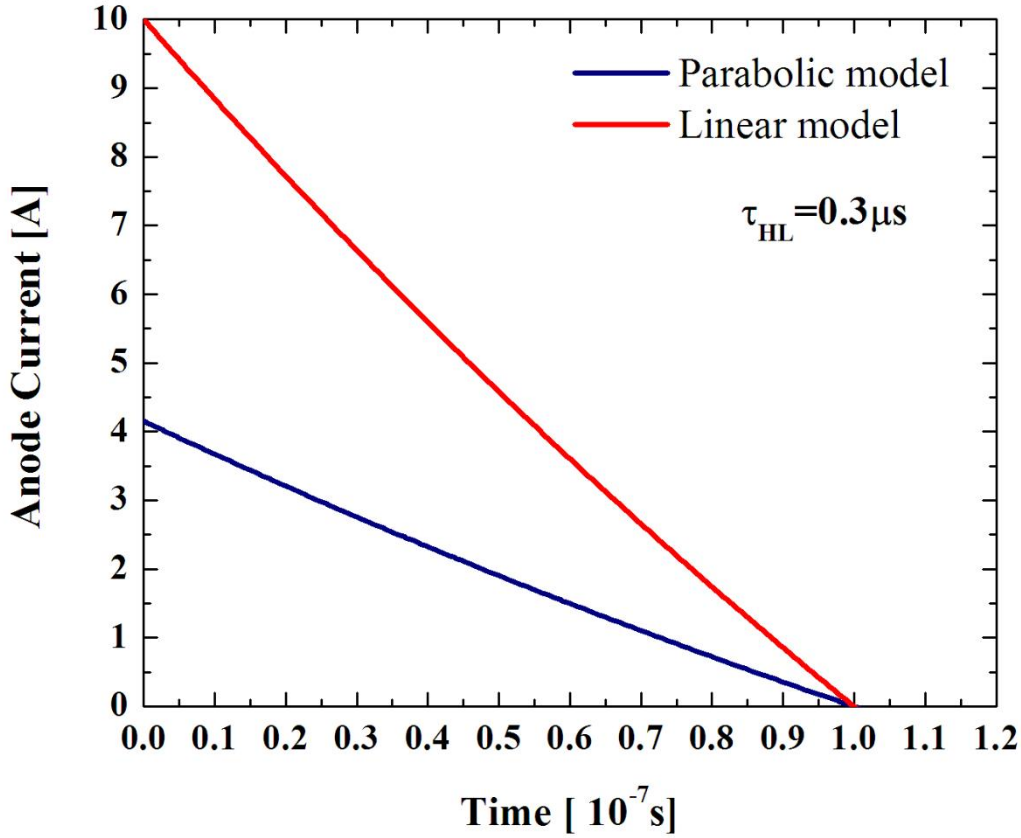

Figure-5.4.3: A comparison between parabolic model and linear model for the anode current for different carrier lifetime(τ_{HL} = 0.3μs)

From figure-5.4.3, it is clear to see the deviation between the two models. Initially the MOSFET gate is turned-off which results rapid withdraw of charges under the gate. This causes instant decay of anode current. After a while the current decrease with a slower rate just likes a BJT. In this case, the parabolic model shows much less current is flowing through IGBT than linear model.

Table 5.4.1: Data Analysis of Transient Anode Current at different carrier lifetime

Carrier Lifetime (μs)	Time (10^{-7}s)	Transient Anode Current (A)		
		Parabolic Model	Linear Model	Difference
High (7.1)	0.00	9.45	10.00	0.547
	0.70	8.31	8.79	0.481
	1.40	7.18	7.59	0.415
	2.10	6.05	6.40	0.350
	2.80	4.94	5.23	0.286
	3.50	3.84	4.06	0.222
	4.20	2.75	2.91	0.159
	4.90	1.67	1.77	0.097
	5.60	0.61	0.64	0.035
Moderate (2.45)	0.00	8.56	10.00	1.440
	0.40	7.49	8.75	1.260
	0.80	6.44	7.52	1.083
	1.20	5.40	6.31	0.909
	1.60	4.38	5.12	0.737
	2.00	3.38	3.95	0.569
	2.40	2.40	2.80	0.403
	2.80	1.43	1.67	0.240
	3.20	0.47	0.55	0.079
Low (0.3)	0.00	4.15	10.00	5.847
	0.12	3.58	8.62	5.038
	0.24	3.03	7.29	4.261
	0.36	2.50	6.01	3.515
	0.48	1.99	4.78	2.797
	0.60	1.50	3.61	2.108
	0.72	1.03	2.47	1.446
	0.84	0.58	1.38	0.810
	0.96	0.14	0.34	0.198

5.5 Simulations for Switching Power Loss:

IGBT switching action is controlled by MOSFET gate voltage. When the turn-off takes place, the gate voltage becomes less than the threshold voltage. The inversion layer at the surface of the P+ body under the gate cannot be kept and that's why zero electron current available in MOSFET. For which, the remaining minority carrier hole stored during the on state of IGBT require some time in order to be removed or extracted. As a result, IGBT sustains high anode current density and voltage simultaneously, which results high power dissipation. This power cannot be used in anywhere else which makes it switching power loss. It is the product of anode voltage and the current. Now, different power profiles for different carrier life times are shown below figures.

A.case: High carrier Lifetime:

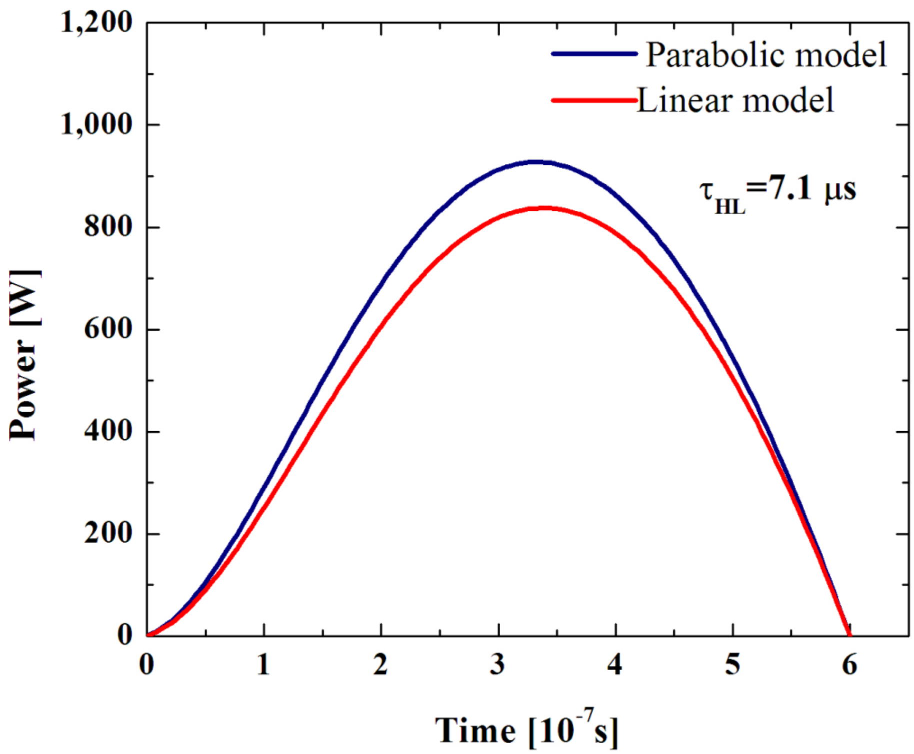

Figure-5.5.1: The instantaneous power dissipated by the IGBT for different Lifetimes (τ_{HL} = 7.1 μs)

The figure shows high carrier lifetime τ_{HL} = 7.1 µs. The previous voltage curve in Figure-5.3.1 and current curve in Figure-5.4.1 shows that, at high carrier life time the current and base charge both is high, whereas the voltage rise gradually compare to other condition. As a result, both current and voltage sustain more time after the turn-off, which result much high power loss compare to other condition during turn-off. The parabolic model provides a more accurate picture of voltage rise and current decay which results in more consistent switching loss compare to linear model.

B.case: Moderate carrier Lifetime:

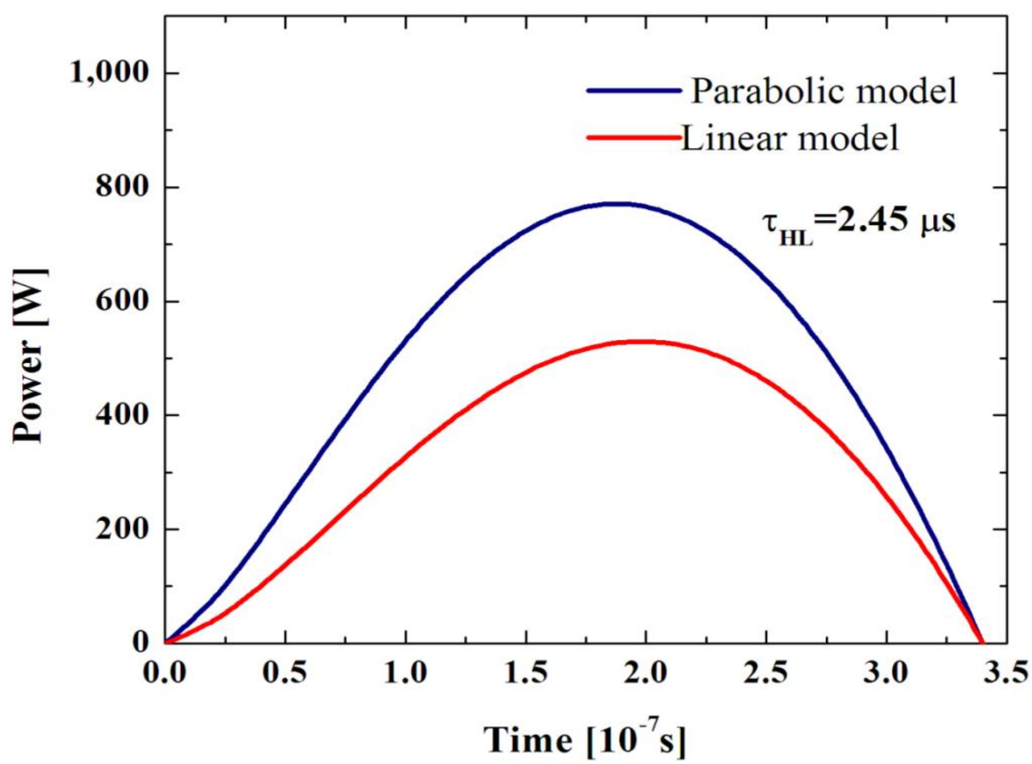

Figure-5.5.2: The instantaneous power dissipated by the IGBT for different Lifetimes (τ_{HL} = 2.45 µs)

In case of τ_{HL} = 2.45 µs both current and voltage sustain less time compare to high carrier life time. This is because only some charge carriers are able to reach collector-base junction before recombination during turn-off. So, a little charge can be built up in the base region which helps the output voltage rise faster than that of in high carrier life time. Besides this, it cause anode current to decay faster. This makes the switching power loss smaller compare to the high carrier life time. In this situation, the power loss in parabolic model is higher compare to the linear model.

C.case : Low carrier Lifetime:

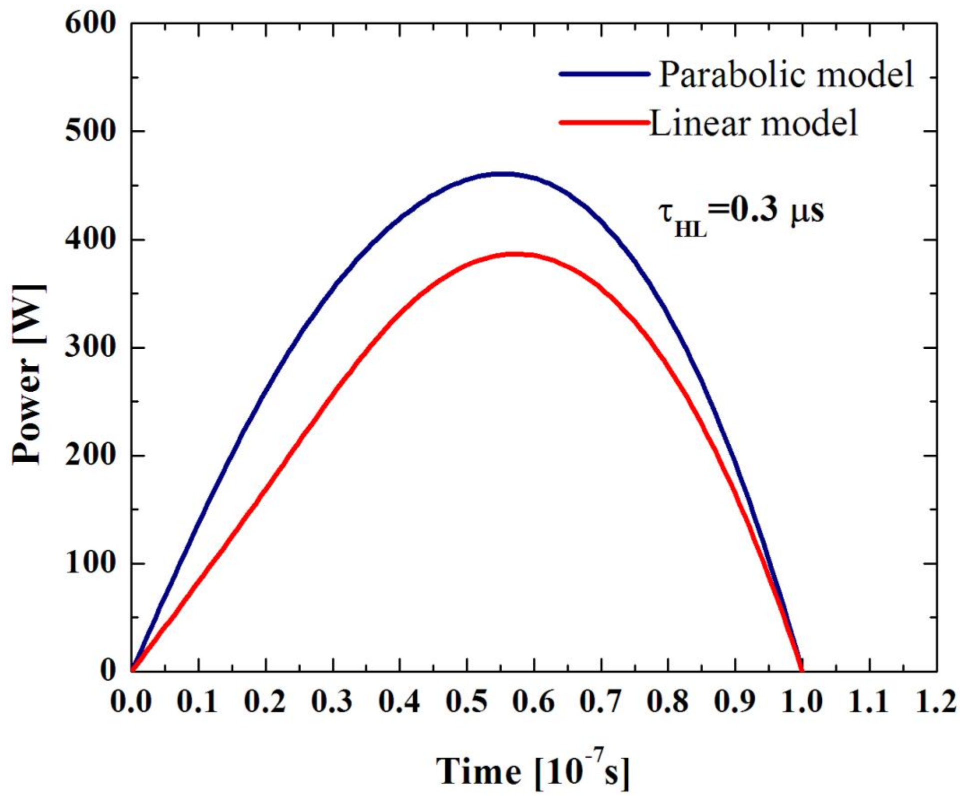

Figure-5.5.3: The instantaneous power dissipated by the IGBT for different Lifetimes (τ_{HL} = 0.3 µs)

Figure 5.5.3 shows that at low currier lifetime, power loss decrease very rapidly. This actually follows the fact that, when carrier lifetime is low, the current as well as charge fall down but the output voltage will rise rapidly. As a result, both voltage and current sustain very little time after turn-off. So, power loss will decrease as it takes less time to turnoff as desired. Here parabolic model switching power loss is higher than linear model.

Table 5.5.1: Data analysis of Switching Power Loss in different carrier lifetime

Carrier Lifetime (µs)	**Time (10^{-7}s)**	**Switching Power Loss (W)**		
		Parabolic Model	**Linear Model**	**Difference**
High (7.1)	0.00	0.00	0.00	0.00
	1.23	388.23	336.33	51.90
	2.46	823.31	731.24	92.08
	3.69	908.53	825.36	83.17
	5.74	158.18	148.00	10.18
Moderate (2.45)	0.00	0.00	0.00	0.00
	0.82	433.68	259.26	174.42
	1.64	752.21	501.66	250.55
	2.46	652.82	470.29	182.53
	3.28	110.06	84.49	25.57
Low (0.3)	0.00	0.00	0.00	0.00
	0.21	265.22	173.16	92.07
	0.41	424.42	337.44	86.98
	0.62	453.65	383.25	70.40
	0.82	305.85	261.54	44.31

Chapter 6

Further scope

In this thesis we have done a lot of analysis with minority carrier concentration, charge, voltage, current and more specifically Switching Power Loss of IGBT at different carrier lifetime. However, many more yet do to further because of time constrain.

For example, a PSPICE IGBT sub circuit can be developed for parabolic model in order to determine I-V characteristics as well as to thoroughly check out the switching characteristics. Moreover forward and reverse breakdown characteristics are also could be determined.

Besides this, greater switching loss often results in hardware damage in IGBT. So, another further work might be: determine & control the power loss which an IGBT can tolerate during turn-off in order to prevent damage and excessive cost.

IGBT is a semiconductor device with combined characteristics of MOSFET & BJT. Which makes switching power loss of IGBT to vary with junction temperatures. So, one can determine the power loss using PSIM simulation.

Bibliography

[1] M. A. Hajji, \ A transient model for insulated gate bipolar transistors (igbts)," September 2002.

[2] V. K. Khanna, Insulated Gate Bipolar Transistor (IGBT) Theory and Design. 445 Hoes Lane, Piscataway, NJ 08854: IEEE Press, 2003.

[3] A. R. Hefner and D. Blackburn, \An analytical model for the steady-state and transient characteristics of the power insulated-gate bipolar transistor," Solid-State Electronics, vol. 31, no. 10, pp. 1513-1532, 1988.

[4] B. J. Baliga, Power Semiconductor Devices. Boston: PWS publishers, 1996.

[5] A. Sattar, Insulated Gate Bipolar Transistor (IGBT) Basics, IXYS Corporation.

[6] A. R. Hefner, \Analytical modeling of device-circuit interactions for the power insulated gate bipolar transistor (igbt)," IEEE Transactions on Industry Applications, vol. 26, no. 06, Nov-Dec 1990.

[7] M. Trivedi and K. Shenai, \Modeling the turn-off of igbts in hard and soft-switching applications," pp. 887-893.

[8] A.Ramamurthy, S.Sawant, and B.J.Baliga, \Modeling the dv/dt of the igbt

during inductive turn-off."

[9] B. Fatemizadeh and D. Silber, \A versatile model for igbt including thermal effects," Seattle, USA, pp. 85-92.

[10] Y.Yue, J. Liou, and I.Batarseh, \A steady-state and transient model valid for all free-carrier injection conditions," 1997.

[11] J.Sgg, P. Tuerkes, and R. Kraus, \Parameter extraction methodology and validation for an electro-thermal physics-based npt igbt model," New Orleans, Louisiana, pp. 1166-1173

[12] D.S.Kuo, C.Hu, and S. Sapp, \An analytical model for the power bipolar mos transistor," pp. 1229-1237.

[13] K. Sheng, S. Finney, and B. Williams, \A new analytical igbt model with improved electrical characteristics," pp. 98-107.

[14] K. Sheng, B. Williams, and S. Finney, \A review of igbt models."

[15] P. Leturcq, \A study of distributed switching processes in igbts and other power bipolar devices," pp. 139-147.

[16] N. Thapar and J. B. Baliga, \An experimental evaluation of the on-state performance of the trench igbt designs."

[17] F. Udrea and G. Amartunga, \An on-state analytical model for the trench igbt."

[18] C. Y. Doo, Y. Kim, M. Han, and Y. Choi, \Numerical analysis of a new vertical igbt structure with reduced jfet effect."
[19] A. L. Robinson, D. N. Pattanayak, Adler, S. Michael, B. J. Baliga, and E. J. Wildi, \Lateral insulated gate transistors with improved latchup characteristics."

[20] M. Darwish and K. Board, \Lateral resurfed comfet," pp. 519-520.

[21] D. N. Pattanayak, A. Robinson, T. P. Chow, S. M. Adler, B. J. Baliga, and E. J. Wildi, \n-channel lateral insulated gate transistors: Part i- steady- state characteristics," pp. 1956-1963.

[22] J. G. Fossum and Y. Kim, \Static and dynamic latchup in the ligbt," pp.1977-1985.

[23] M. Vellvehi, P. Godignon, D. Flores, J. Fernandez, S. Hidalgo, J. Rebollo, and J. Millan, \A new lateral igbt for high temperature operation," pp. 739-747.
[24] S. Ravishankar and B. J. Baliga, \Analysis of on-state carrier distribution in the di-ligbt," pp. 733-738.
[25] H. Qun and A. Gehan, \Forward blocking capability of double gate igbts at high temperatures," pp. 981-982.

Appendix A

Steady state charge control

Ambipolar Diffusion equation in Base

$$\frac{\partial^2 p(x)}{\partial x^2} - \frac{p(x)}{L^2} = 0 \tag{A.1}$$

Boundary conditions:

$$p(x = 0) = P_0$$

$$p(x = W) = 0$$

Minority carrier concentration in n base region on IGBT is

$$p(x) = Ae^{\frac{x}{L}} + Be^{-\frac{x}{L}} \tag{A.2}$$

Now at, $x = 0$

$$p(0) = A + B$$

$$P_0 = A + B$$

(A.3)

Now at, $x = w$

$$0 = p(x) = Ae^{\frac{W}{L}} + Be^{-\frac{W}{L}}$$

(A.4)

Now multiplying $e^{-\frac{W}{L}}$ to the equation (A.3), we get

$$Ae^{-\frac{W}{L}} + Be^{-\frac{W}{L}} = P_0 e^{-\frac{W}{L}}$$

(A.5)

Subtracting (A.5) from (A.4), we get A

$$A\left(e^{\frac{W}{L}} + e^{-\frac{W}{L}}\right) = -P_0 e^{-\frac{W}{L}}$$

$$A = \frac{-P_0 e^{-\frac{W}{L}}}{2j\,\sinh\left(\frac{W}{L}\right)}$$

(A.6)

Again we multiply equation (A.3) with $e^{\frac{W}{L}}$

$$Ae^{\frac{W}{L}} + Be^{\frac{W}{L}} = P_0 e^{\frac{W}{L}} \qquad \text{(A.7)}$$

Subtracting (A.7) from (A.4), we find out B

$$B\left(e^{\frac{W}{L}} - e^{-\frac{W}{L}}\right) = P_0 e^{\frac{W}{L}}$$

$$B = \frac{P_0 e^{\frac{W}{L}}}{2j\,\sinh\left(\frac{W}{L}\right)} \qquad \text{(A.8)}$$

So, the total solution would be

$$p(x) = \frac{-P_0 e^{-\frac{W}{L}}}{2j\,\sinh\left(\frac{W}{L}\right)} e^{\frac{x}{L}} + \frac{P_0 e^{\frac{W}{L}}}{2j\,\sinh\left(\frac{W}{L}\right)} e^{-\frac{x}{L}}$$

(A.9)

$$= P_0 \frac{e^{\frac{W-x}{L}} - e^{-\frac{(W-x)}{L}}}{2j\,\sinh\left(\frac{W}{L}\right)}$$

$$p(x) = P_0 \frac{\sinh\left(\frac{W-x}{L}\right)}{\sinh\left(\frac{W}{L}\right)}$$

(A.10)

Now, integrating p(x), we get the total steady state excess base charge

$$Q_0 = qA \int_0^W p(x)dx$$

$$Q_0 = qA \frac{P_0}{\sinh\left(\frac{W}{L}\right)} \int_0^W \sinh\left(\frac{W-x}{L}\right) dx$$

Let,

$$\frac{W-x}{L} = z$$

Differentiating

$$\frac{-1}{L}dx = dz$$

$$dx = -Ldz$$

Boundary Limits:

x=0 $\quad z = \frac{W}{L}$

x=W $\quad z = 0$

so,we get

$$Q_0 = qA\frac{P_0}{\sinh\left(\frac{W}{L}\right)}\int_{\frac{W}{L}}^{0}\sinh(-L)\sinh z dz$$

$$= \frac{qAP_0L}{\sinh\left(\frac{W}{L}\right)}\left[\cosh z\right]_0^{\frac{W}{L}}$$

$$= \frac{qAP_0L}{\sinh\left(\frac{W}{L}\right)}\left[\cosh\left(\frac{W}{L}\right) - 1\right]$$

We know,

$$\cosh(2x) = 1 + 2sinh^2(x) \qquad \text{(A.11)}$$

$$\sinh(2x) = 2\sinh(x)\cosh(x) \qquad \text{(A.12)}$$

The total excess base charge

$$Q_0 = qAP_0L\frac{2sinh^2\left(\frac{W}{2L}\right)}{2\sinh\left(\frac{W}{2L}\right)\cosh\left(\frac{W}{2L}\right)}$$

$$Q_0 = qAP_0L\tanh\left(\frac{W}{2L}\right) \qquad \text{(A.13)}$$

Appendix B

Linear Charge Control

From the steady state analysis, we have

$$p(x) = P_0 \frac{\sinh\left(\frac{W-x}{L}\right)}{\sinh\left(\frac{W}{L}\right)} \qquad \text{(B.1)}$$

Since the diffusion length (L) is larger than the drift layer thickness (W_B) because of the high lifetime of the carriers, one can approximate the carrier profile for the holes p(x) in the drift layer by a linear expression as shown previously

$$p(x,t) = P_0\left[1 - \frac{x}{W(t)}\right] \qquad \text{(B.2)}$$

With the aid of the general ambipolar transport hole current expression

$$I_p = \frac{1}{1+b} I_T(t) - qAD\,\frac{\partial p\,(x)}{\partial x} \qquad \text{(B.3)}$$

We can find an expression for P_0 from equations (B.2) & (B.3) as

$$\frac{\partial p\,(x)}{\partial x} = -\frac{P_0}{W(t)} \qquad \text{(B.4)}$$

As

$$I_n(0) = 0$$

So

$$I_p(0) = I_T(t)$$

And

$$I_p(0) = I_T(t) = \frac{I_T(t)}{1+b} + \frac{2qAD_P}{1+\frac{1}{b}}\frac{P_0}{W(t)}$$

$$I_T(t)\left[1 - \frac{1}{1+b}\right] = \frac{2qAD_P}{1+\frac{1}{b}}\frac{P_0}{W(t)}$$

$$I_T(t) = I_T(t=0) = I_T(0^-)$$

$$P_0 = \frac{W(t)I_T(0^-)}{2qAD_P} \qquad \text{(B.5)}$$

Since total anode current is constant $I_T(t) = I_T(0^-)$, from the above equation we can find $\frac{\partial P_0}{\partial t}$ as

$$\frac{\partial P_0}{\partial t} = \frac{W(t)I_T(0^-)}{2qAD_P}\frac{d}{dt}W(t)$$

Substituting for $I_T(0^-)$ from equation (B.5), the above equation becomes

$$\frac{\partial P_0}{\partial t} = -\frac{P_0}{W(t)}\frac{d}{dt}W(t) \qquad \text{(B.6)}$$

From Figure (3.3) the slope is negative since the behaviour of $W(t)$ tends towards the minus x direction as the device voltage $V_{CE}(t)$ varies with time (moving boundary). The total excess charge in the base of the IGBT is

$$Q(t) = qAP_0 \int_0^W \left[1 - \frac{x}{W(t)}\right] dx$$

$$= qAP_0 \left[x - \frac{x^2}{2W(t)}\right]_0^W$$

$$= qAP_0 \left[W(t) - \frac{W(t)^2}{2W(t)}\right]$$

$$= qAP_0 \left[W(t) - \frac{W(t)}{2}\right]$$

$$= qAP_0 \frac{W(t)}{2} \qquad \text{(B.7)}$$

$$Q(t) = qA\frac{W(t)}{2}\frac{W(t)I_T(t)}{2qAD_P}$$

$$I_T(t) = \frac{4D_P}{W(t)^2}Q(t) \qquad \text{(B.8)}$$

Equation (B.8) is the linear charge control current and W is a constant in this case since $\frac{dV_{CE}}{dt} = 0$

Appendix C

Effective Depletion width from Poisson's Equation

[27] An electric field is created in the depletion region by the separation of positive and negative space charge densities. Fig. C.1 shows the volume charge density distribution in the pn junction assuming uniform doping and assuming an abrupt junction approximation. We will assume that the space charge region abruptly ends in the n region at $x = +x_n$,and abruptly ends in the p region at$x = -x_p$, (x_p is a positive quantity).

The electric field is determined from Poisson's equation which, for a one-dimensional analysis, is

$$\frac{d^2\emptyset(x)}{dx^2} = \frac{-\rho}{\epsilon_s} = -\frac{dE(x)}{dx} \qquad \text{(C.1)}$$

Where $\emptyset(x)$ is the electric potential, $E(x)$is the electric field, $\rho(x)$is the volume charge density and ϵ_s is the permittivity of the semiconductor. From Fig. D.1, the charge densities are

$$\rho(x) = -eN_a \qquad -x_p < x < 0 \qquad \text{(C.2)}$$

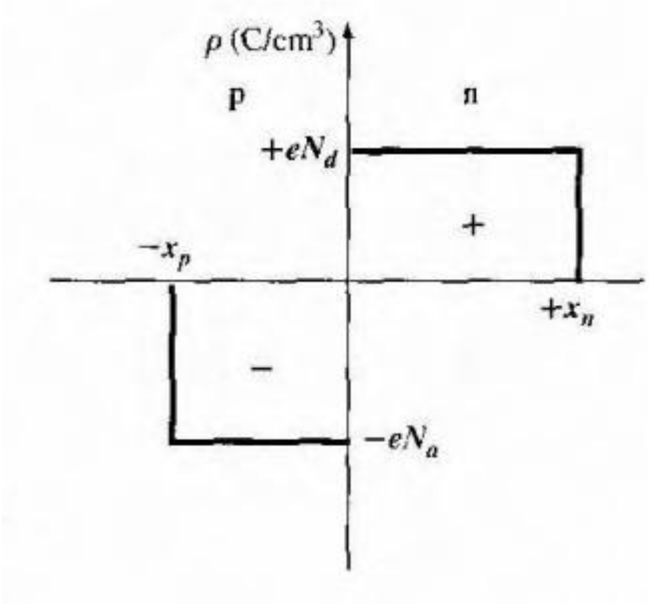

Figure C.1: The space charge density in a uniformly doped pn junction assuming the abrupt junction approximation

and,

$$\rho(x) = -eN_d \qquad 0 < x < x_n \qquad \text{(C.3)}$$

The electric field in the p region is found by integrating Equation (C.1), We have that

$$E = \int \frac{\rho(x)}{\epsilon_s} dx = -\int \frac{eN_a}{\epsilon_s} dx = -\frac{eN_a}{\epsilon_s} x + C_1 \qquad \text{(C.4)}$$

Where C_1 is a constant of integration. The electric field is assumed to be zero in the neutral p region for $x < x_p$, since the currents are zero in thermal equilibrium. As there are no surface charge densities within the pn junction structure, the electric field is a continuous function. The constant of integration is determined by setting
$E = 0$ at $x = x_p$. The electric field in the p region is then given by

$$E = -\frac{eN_a}{\epsilon_s}(x + x_p) \qquad -x_p \le x \le 0 \qquad \text{(C.5)}$$

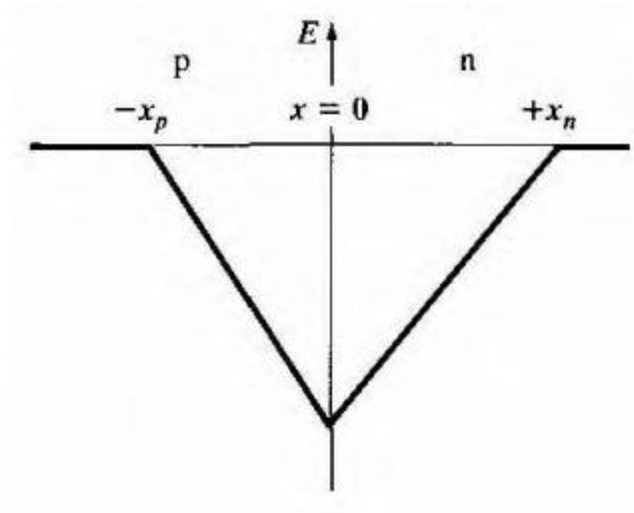

Figure C.2: Electric field in the space charge region of a uniformly doped pn junction

Then the n region, the electric field is determined from

$$E = \int \frac{eN_d}{\epsilon_s} dx = \frac{eN_d}{\epsilon_s} x + C_2 \qquad \text{(C.6)}$$

Where C_2 is again a constant of integration. The constant C_2 is determined by setting $E = 0$ at $x = x_n$, since the Electric field is assumed to be zero in the n region and is a continuous function. Then

$$E = -\frac{eN_a}{\epsilon_s}(x_n - x) \qquad 0 \leq x \leq x_n \qquad \text{(C.7)}$$

The electric field is also continuous at the metallurgical junction, or at $x = 0$.Setting Equations (C.5) and (C.7) equal to each other at $x = 0$ gives

$$N_a x_p = N_d x_n \qquad \text{(C.8)}$$

Equation (C.8) states that the number of negative charges per unit area in the p region is equal to the number of positive charges per unit area in the n region.

Fig. C.2 is a plot of the electric field in the depletion region. The electric field direction is from the n to the p region, or in the negative x direction for this geometry. For the uniformly doped pn junction, the Electric field is a linear function of distance through the junction, and the maximum (magnitude) electric field occurs at the metallurgical junction. An electric field exists in the depletion region even when no voltage is applied between the p and n regions.

The potential in the junction is found by integrating the electric field. In the p region then, we have

$$\emptyset(x) = -\int E dx = \int \frac{eN_a}{\epsilon_s}(x + x_p)dx \qquad \text{(C.9)}$$

$$\emptyset(x) = \frac{eN_a}{\epsilon_s}\left(\frac{x^2}{2} + x_p\right) + C_1' \qquad \text{(C.10)}$$

where C_1' is again a constant of integration. The potential difference through the pn junction is the important parameter, rather than the absolute potential, so we may arbitrarily set the potential equal to zero at $x = -x_p$. The constant of integration is then found as

$$C_1' = \frac{eN_a}{2\epsilon_s}{x_p}^2 \qquad \text{(C.11)}$$

so that the potential in the p region can now be written as

$$\emptyset(x) = \frac{eN_a}{2\epsilon_s}\left(x + x_p\right)^2 \qquad -x_p \leq x \leq 0 \qquad \text{(C.12)}$$

The potential in the region is determined by integrating the electric field in the n region, or

$$\emptyset(x) = -\int E dx = \int \frac{eN_d}{\epsilon_s}(x_n - x)dx \qquad \text{(C.13)}$$

Then

$$\emptyset(x) = \frac{eN_d}{\epsilon_s}\left(x_n x - \frac{x^2}{2}\right) + C_2' \qquad \text{(C.14)}$$

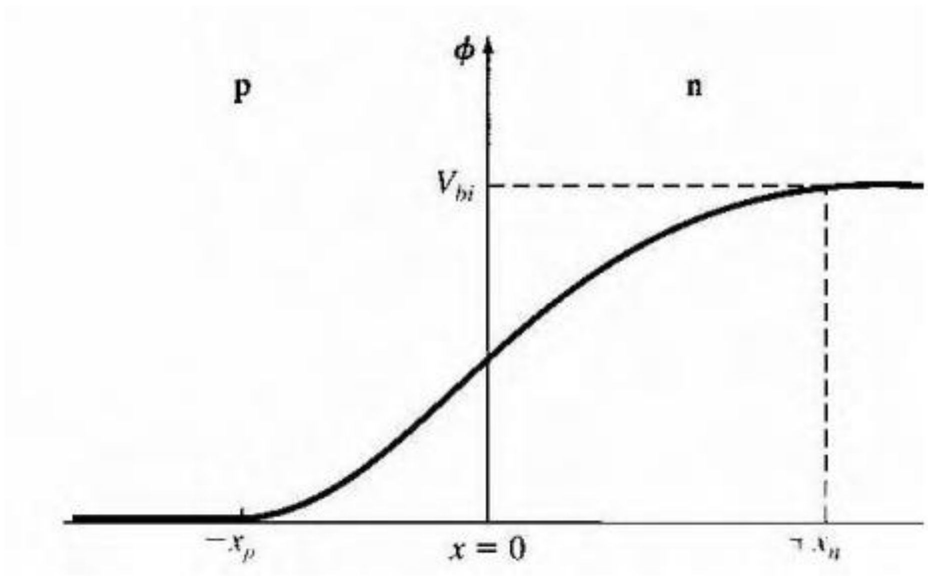

Figure C.3: Electric Potential through the space charge region of a uniformly doped pn junction

where C_2' is another constant of integration. The potential is a continuous function, so setting Equation (7.21) equal to Equation (C.14) at the metallurgical junction, or at x = 0, gives

$$C_2' = \frac{eN_a}{2\epsilon_s} x_p^2 \qquad \text{(C.15)}$$

The potential in then region can thus be written as

$$\emptyset(x) = \frac{eN_d}{\epsilon_s}\left(x_n x - \frac{x^2}{2}\right) + \frac{eN_a}{2\epsilon_s} x_p^2 \qquad 0 \le x \le x_n \qquad \text{(C.16)}$$

Fig. C.3 is a plot of the potential through the junction and shows the quadratic dependence on distance. The magnitude of the potential at $x = x_n$ is equal to the built-in potential barrier. Then from Equation (C.16), we have

$$V_{bi} = [\emptyset(x = x_n)] = \frac{e}{2\epsilon_s}\left(N_a x_p^2 + N_d x_n^2\right) \qquad \text{(C.17)}$$

We can determine the distance that the space charge region extends into the p and n regions from the metallurgical junction. This distance is known as the space charge width or Depletion Width. From Equation (C.8), we may write;

For example

$$x_p = \frac{N_d x_n}{N_a} \qquad \text{(C.18)}$$

Then, substituting Equation (C.18) into Equation (C.17) and solving for x, we obtain

$$x_n = \left\{\frac{2\epsilon_s V_{bi}}{e}\left(\frac{N_a}{N_d}\right)\left(\frac{1}{N_a+N_d}\right)\right\}^{\frac{1}{2}} \qquad \text{(C.19)}$$

Equation (C.19) gives the space charge width or the width of the depletion region, x_n,extending into the n-type region for the case of zero applied voltage.

Similarly, if we solve for x_n from Equation (C.8) and substitute into Equation (C.17), we find

$$x_p = \left\{\frac{2\epsilon_s V_{bi}}{e}\left(\frac{N_d}{N_a}\right)\left(\frac{1}{N_a+N_d}\right)\right\}^{\frac{1}{2}} \qquad \text{(C.20)}$$

Where x_p is the width of the depletion region extending into the p region for the case of zero applied voltage.

The total depletion or space charge width W is the sum of the two components, or

$$W_{depletion} = x_n + x_p \qquad \text{(C.21)}$$

Using Equations (C.19) and (C.20), we obtain

$$W_{depletion} = \left\{\frac{2\epsilon_s V_{bi}}{e}\left(\frac{N_a+N_d}{N_a N_d}\right)\right\}^{\frac{1}{2}} \qquad \text{(C.22)}$$

In case of collector-base region of the IGBT, the collector is highly doped p^+ region, whether the base is lightly doped n^-. So we can say $N_d << N_a$. From equation (C.8) we see

$$x_n >> x_p \tag{C.23}$$

and

$$x_n \approx W_{bcj} \tag{C.24}$$

where $W_{bcj} = W_{depletion}$. Here V_{bi}=V_{CE} (collector-emitter voltage), q=e (electron charge) and N_d=N_b (base impurity concentration). So the base-collector depletion width reduces to

$$W_{bcj} = \left\{\frac{2\epsilon_s V_{CE}(t)}{qN_B}\right\}^{\frac{1}{2}} \tag{C.25}$$

If the metallurgical base width is W_B, then the effective depletion width can be written as

$$W(t) = W_B - W_{bcj}(t)$$

$$W(t) = W_B - \sqrt{\left\{\frac{2\epsilon_s V_{CE}(t)}{qN_B}\right\}} \tag{C.26}$$

Appendix D

Ambipolar Diffusion Coefficient

At high injection levels, electrons and holes transport cannot be treated separately because the electrons move in a cloud of holes and conversely. A convenient approach to handle this situation involves combination of continuity equation for electrons with that for holes, and introduction of a new parameter, namely, Ambipolar Diffusion Coefficient, which is an algebraic function of electron and hole diffusivities and concentrations. The defining equation for the ambipolar diffusion coefficient is

$$D = \frac{nq\,\mu_n D_p + pq\,\mu_p D_n}{nq\,\mu_n + pq\,\mu_p}$$

Where,

D_n =Electron Diffusion Coefficient

D_p = Hole Diffusion Coefficient

μ_n = Electron mobility

μ_p = Hole mobility

n = electron concentration

p = hole concentration

q = charge

The advantage gained from this approach is that the resulting single equation allows focusing our attention on the minority carrier concentration, while the presence of majority carrier concentration is automatically accounted for by the ambipolar diffusion coefficient.

Now, we know from Eienstein's Equation

$$\frac{D_n}{\mu_n} = \frac{kT}{q}$$

$$\frac{D_p}{\mu_p} = \frac{kT}{q}$$

$$\frac{D_n}{D_p} = \frac{\mu_n}{\mu_p} = b$$

Assuming $n = p$

$$D = \frac{nq\left(\mu_n D_p + \mu_p D_n\right)}{nq\left(\mu_n + \mu_p\right)}$$

$$= \frac{\left(\mu_n D_p + \mu_p D_n\right)}{\left(\mu_n + \mu_p\right)}$$

$$= \frac{\left(\frac{\mu_n}{\mu_p} D_p + D_n\right)}{\left(\frac{\mu_n}{\mu_p} + 1\right)}$$

$$= \frac{b D_p + D_n}{b + 1}$$

$$= \frac{D_p + \frac{D_n}{b}}{1 + \frac{1}{b}}$$

$$= \frac{D_p + D_n \frac{D_p}{D_n}}{1 + \frac{1}{b}}$$

$$= \frac{2D_p}{1 + \frac{1}{b}}$$

So, $$D\left(1 + \frac{1}{b}\right) = 2D_p \qquad \text{(D.1)}$$

Appendix E

Fourth order RUNGE-KUTTA

(RK4) method

Fourth order Runge-Kutta (RK4) method is a numerical technique used to solve ordinary differential equation of the form:

$$\frac{dy}{dx} = f(x, y), \; y(0) = y_0$$

So only first order ordinary differential equations can be solved by using the Runge - Kutta 4th order method.

The most commonly used set of values leads to the procedure:

$$y_{n+1} = y_n + \frac{1}{6}(k_1 + 2k_2 + 2k_3 + k_4)$$

$$k_1 = hf(x_n, y_n)$$

$$k_2 = hf\left(x_n + \frac{1}{2}h, y_n + \frac{1}{2}k_1\right)$$

$$k_3 = hf\left(x_n + \frac{1}{2}h, y_n + \frac{1}{2}k_2\right)$$

$$k_4 = hf(x_n + h, y_n + k_3)$$

The local error term for the fourth-order Runge-Kutta method is

$$(oh^4)$$

The global error would be

$$(oh^4)$$

It is computationally more efficient than the modified Euler method because, although four evaluations of the function are required per step rather than two, the steps can be many-fold larger for the same accuracy. The Runge-Kutta techniques have been very popular, especially the forth order method just presented. Because going from two to fourth order was so beneficial, we may wonder whether we should use a still higher order formula. Higher order (fifth, sixth and so on) Runge-Kutta formulas have been developed and can be used to advantage in determining a suitable size for h. Still, Runge-Kutta methods of order greater than four have the disadvantage that the number of function evaluations that are required is greater than the order than the method, while Runge-Kutta method of order 4 require the same number of evaluations as the order.

It is important to keep in mind that there are three possible sources of error in numerical calculations, such as solutions to ordinary differential equations. The one we have discussed the most is truncation error, the error associated with the number of terms in a series, e.g. Taylor series. Other sources of error are round-off errors, which will always be present even if our method is exact, and original data errors, associated with not knowing the initial conditions or boundary conditions exactly [see Box 3.1]. Errors at each step propagate through the solution, so the global error is generally about an order larger than the local error. A method is convergent if the approximate solution tends toward the true solution as

$$\Delta x \to 0$$

All of the widely used methods for solving ordinary differential equations (in particular the ones we have discussed) are convergent. Stability refers to the growth of errors as the solution proceeds. A stable method is one in which the global error does not grow in an unbounded manner. For many ODE's, the step size required to obtain an accurate solution is much smaller than the step size required for stability. As a result, stability is often not a major concern. When a solution is unstable, it is usually obvious. A smaller step size will generally rectify the problem, although there are cases that are unconditionally unstable for some methods. Changing methods is the best approach in such cases.